NASA TECHNICAL NOTE

NASA TN D-2427

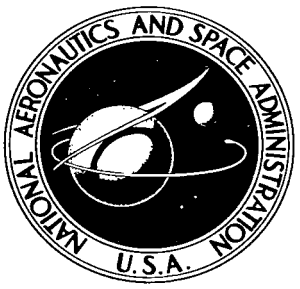

NASA TN D-2427

EFFECT OF AIR INJECTION THROUGH A POROUS SURFACE AND THROUGH SLOTS ON TURBULENT SKIN FRICTION AT MACH 3

by Donald I. McRee, John B. Peterson, Jr., and Albert L. Braslow

Langley Research Center
Langley Station, Hampton, Va.

NATIONAL AERONAUTICS AND SPACE ADMINISTRATION • WASHINGTON, D. C. • AUGUST 1964

EFFECT OF AIR INJECTION THROUGH A POROUS SURFACE AND THROUGH SLOTS ON TURBULENT SKIN FRICTION AT MACH 3

By Donald I. McRee, John B. Peterson, Jr.,
and Albert L. Braslow

Langley Research Center
Langley Station, Hampton, Va.

NATIONAL AERONAUTICS AND SPACE ADMINISTRATION

For sale by the Office of Technical Services, Department of Commerce,
Washington, D.C. 20230 -- Price $1.00

EFFECT OF AIR INJECTION THROUGH A POROUS SURFACE AND THROUGH SLOTS ON TURBULENT SKIN FRICTION AT MACH 3

By Donald I. McRee, John B. Peterson, Jr.,
and Albert L. Braslow
Langley Research Center

SUMMARY

A preliminary investigation has been made at a free-stream Mach number of 3 and a free-stream Reynolds number per foot of 9.75×10^6 of the effectiveness of injection of air into the boundary layer through a porous surface and through single rearward-inclined slots in reducing the level of supersonic turbulent skin friction. Local and average skin-friction coefficients are presented for each injection configuration. The boundary-layer profiles are also shown and compared with the standard 1/7-power turbulent profile. A reduction in the average turbulent skin-friction coefficient of approximately 20 percent was obtained by distributed air injection through a porous surface. The most effective slot configuration investigated was the narrowest flush slot (0.018 inch wide), which provided a reduction in average skin-friction coefficient of 10 to 15 percent. All other slot configurations resulted in an increase in skin friction with increased injection rate. The effectiveness of the various slot configurations appears to be largely dependent on the manner in which the injected air mixes with the original boundary layer.

Although the distributed air injection resulted in a greater decrease in skin friction than the rearward-inclined slots, other considerations such as momentum recovery of the injection air must be considered before a conclusion can be made as to which type of injection is the most effective in reducing overall drag.

INTRODUCTION

Turbulent skin-friction drag is a large portion of the total drag of slender aircraft. Any method that offers a possibility of reducing the level of the turbulent skin friction, therefore, warrants investigation. Theory and experiment (refs. 1 to 5) have shown that distributed injection of air or a light gas into the boundary layer through a porous surface will significantly decrease the skin friction, with greater reductions attainable with the use of light gases for the same mass flow. Calculations have shown, however, that the drag reductions attainable with the light gases are not great enough to compensate for the fuel energy used in accelerating the gas weight to cruise speed.

Use of air taken on board the aircraft during flight for other purposes, however, offers an interesting possibility for reducing drag.

Inasmuch as injection of air through large areas of porous surface is impractical at present from a structural standpoint, this investigation was initiated to study the effectiveness of injection of air through individual slots in reducing skin friction. A porous surface was tested for comparison with the slot-injection results. Should the injection of air through a slot thicken the boundary layer without appreciably distorting the nondimensional velocity profile, a reduction in local skin friction would be attainable. If, however, the thickening of the boundary layer is accompanied by a distortion of the profile such that the velocity slope at the surface is increased, an increase in local skin friction would occur. Inasmuch as the mixing effects on the profile shape cannot be calculated, experimentation must be relied upon to develop an efficient slot configuration.

A preliminary investigation has been made of air injection through a few individual slot configurations near the leading edge of a flat-plate model at a free-stream Mach number of 3 in the Langley 20-inch variable supersonic tunnel. The tests were made at a free-stream Reynolds number per foot of 9.75×10^6 through a range of air-injection flow rates. Both average and local skin-friction coefficients were evaluated at a position approximately 20 inches downstream of the plate leading edge.

SYMBOLS

$C_{D,meas}$ drag coefficient obtained from momentum thickness, $\frac{2\theta}{x_v}$

$C_{D,air}$ drag coefficient obtained by taking free-stream air on board and bringing it to rest, $\frac{\dot{m}U_\infty}{\frac{1}{2}\rho_\infty U_\infty^2 S}$, or $2F$

C_f local skin-friction coefficient

C_F average skin-friction coefficient

C_T thrust coefficient, $\frac{\text{Thrust}}{q_\infty S}$

$F = \frac{\dot{m}}{\rho_\infty U_\infty S}$

$\frac{2F}{C_{F,o}}$ mass-flow parameter

l span of slot

$\dot{m}$	injection mass-flow rate
q	dynamic pressure
S	reference area, $x_v l$
u	velocity
U_∞	free-stream velocity
w	width of slot
x	distance measured from leading edge along axis of plate
x_v	distance measured from virtual origin of turbulence along axis of plate
y	perpendicular distance from plate
δ	boundary-layer thickness
θ	momentum thickness of boundary layer
ϕ	inclination of slot, $\phi = 15^\circ$
ρ	density

Subscripts:

∞	free-stream conditions
o	solid flat plate

APPARATUS

Wind Tunnel

The investigation was conducted in the Langley 20-inch variable supersonic tunnel which is an intermittent blowdown-type wind tunnel. Flexible nozzle walls, actuated by hydraulic motors, are used to vary the Mach number from 2.0 to 4.5. A schematic diagram of the tunnel is presented in figure 1. The maximum stagnation pressure attainable is 125 pounds per square inch absolute. Electrical resistance-type air heaters are available to prevent air liquefaction at the higher Mach numbers and to maintain a constant stagnation temperature, when desired, at the lower Mach numbers.

Model

The test model was a sharp-leading-edge (radius of 0.0075 inch to 0.007 inch) flat-plate configuration mounted vertically on a strut off the sidewall of the tunnel. A photograph of the model as viewed through the opposite tunnel window is presented as figure 2.

Three basic configurations consisting of a solid surface, a sintered-bronze porous surface of uniform porosity and a slotted surface were investigated. (See fig. 3.) The porous surface was 14 inches wide and extended from 3 to 19 inches from the plate leading edge. Each of the slots was also 14 inches in span and was located about 3 inches from the leading edge. Two different slot types were investigated: rearward-inclined flush slots and rearward-inclined step slots, both of which were inclined 15° to the direction of flow. Flush slots with widths of 0.018, 0.040, 0.065, and 0.089 inch and a step slot with a width of 0.068 inch were tested. The width was measured as indicated in figure 3. The model assembly for the flush-slot configuration is shown in figure 4.

A boundary-layer trip consisting of distributed three-dimensional roughness (No. 60 carborundum) was placed 1 inch from the leading edge of all configurations to insure turbulent flow over the models. Reference 6 was used to calculate the height of roughness required to trip the boundary layer.

Instrumentation

The solid-surface configuration and the slotted configurations were equipped with four static-pressure orifices on the surface of the model located 12, 16, 18, and 20 inches from the leading edge (fig. 4). The porous configuration had only one static orifice on the upper surface located 20 inches from the leading edge. The slot configurations contained three total-pressure tubes in the entrance to the slot to observe the spanwise uniformity of the flow through the slots (fig. 4). The total-pressure measurements indicated that the injected air entered the slot uniformly for all injection rates. Located in the plenum chamber for all configurations were a total-pressure tube to measure chamber total pressure and a thermocouple to measure chamber total temperature. A total-pressure boundary-layer survey apparatus was mounted opposite the model surface as shown in figure 2. This apparatus allowed the movement of a total-pressure probe approximately $10\frac{1}{2}$ inches in the streamwise direction and 1 inch normal to the model surface. The thickest boundary layer encountered was approximately one-half inch. The height of the boundary-layer survey probe from the plate surface could be recorded to an accuracy of 0.0005 inch. A close-up photograph and a schematic drawing of the survey probe are presented in figures 5(a) and 5(b), respectively.

The air for injection was taken from the main airstream by a pickup pipe mounted through the wall of the tunnel downstream of the model. This air was then piped through a line containing a venturi to the plenum chamber. Measurements were made of venturi total pressure, venturi differential pressure, and venturi total temperature in order to calculate the mass flow passing into the model.

A local-skin-friction balance having a 1-inch-diameter floating disk, similar to those used in reference 7, was mounted 20 inches from the leading edge of all configurations. The load range of the skin-friction balance used was 0 to 0.029 pound.

PROCEDURE

All tests were made at a free-stream Mach number of 3.0 and a free-stream Reynolds number per foot of 9.75×10^6. The tunnel stagnation pressure was 60 pounds per square inch absolute and the stagnation temperature was 70° F. The total temperature of the injected air was approximately 50° F. The mass rate of flow of the injected air ranged from 0 to 0.061 pound per second. This flow rate, in terms of the nondimensional mass-flow parameter $2F/C_{F,o}$, ranged from 0 to 0.85. The mass-flow rate was regulated by use of a valve located between the venturi and the model. The solid-surface configuration was first tested to determine the turbulent solid-plate local and average skin-friction coefficients. Boundary-layer profiles were measured on the solid configuration at 12.0, 14.0, 16.0, and 19.325 inches from the leading edge. The static pressure at a particular station was used in the reduction of the survey data at that station to the desired form. On the porous and slot configurations, a boundary-layer survey was made only at 19.325 inches from the leading edge. At this station the static pressure was equal to the free-stream static pressure for all cases. A constant total temperature through the boundary layer was assumed in reducing all the data. This assumption appears to be reasonable for the slot-injection cases since only approximately 4 percent of the air in the boundary layer passing the survey probe is injected air for the highest mass-flow rate. All the local skin-friction data presented were obtained from the skin-friction balance except for a few points obtained on the solid plate from the slope of θ with x. The center of the skin-friction balance was located at the 20-inch station. The measurements of the skin-friction balance were taken after the boundary-layer surveys were completed and the probe was moved downstream of the balance. The reference area used to reduce the force data of the balance to coefficient form was the area of the floating disk plus one-half of the area of the gap around the disk, as was used in reference 8. For the present investigation, this area was 0.7949 square inch.

RESULTS AND DISCUSSION

All experimental data were reduced in such a manner as to permit determination of the effect of air injection on local and average turbulent skin-friction coefficients. In order to obtain the average turbulent skin-friction coefficient, the experimentally measured momentum thickness must be separated into contributing components. Not only does the momentum thickness θ include momentum losses due to skin-friction drag but also any other drag inputs which take place ahead of the survey station. The following sketch illustrates the

components involved and how the desired average skin-friction coefficients were obtained from the measurements of θ.

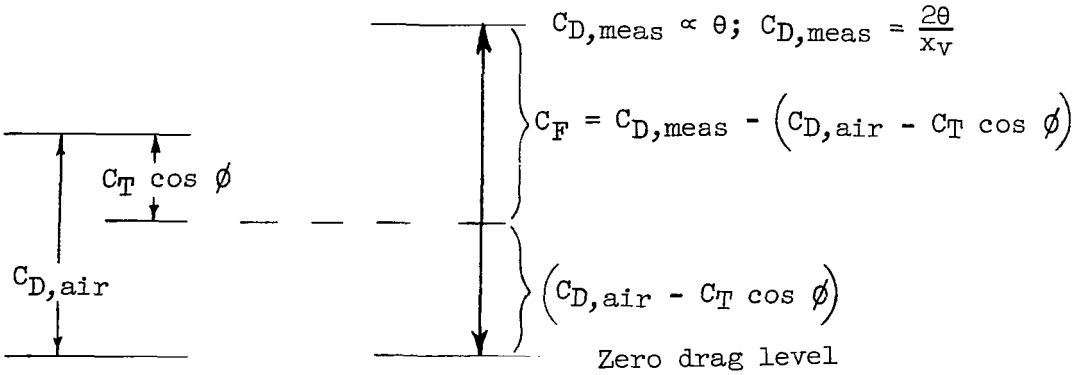

From the measured momentum thickness θ a drag coefficient $C_{D,meas}$ was obtained. For air injection normal to the plate surface, as in the case of the distributed injection, this drag coefficient includes not only the plate skin friction but also the complete momentum defect from free-stream conditions of the injected air, represented as $C_{D,air}$. For injection through rearward-inclined slots, some of the momentum loss is recovered and is defined in terms of a thrust coefficient C_T. This thrust coefficient was calculated by using the measured mass flow and chamber total pressure and temperature. From these measured values, the slot Mach number and slot pressure were obtained. By using these conditions, the thrust in the stream direction $C_T \cos \phi$ was calculated. For the slot tests, then, the momentum defect in the injected air is $\left(C_{D,air} - C_T \cos \phi\right)$. This momentum defect will show up in the boundary layer at the survey station and therefore must be subtracted from $C_{D,meas}$ in order to obtain the average skin-friction coefficient, that is,

$$C_F = C_{D,meas} - \left(C_{D,air} - C_T \cos \phi\right)$$

Solid Plate

Boundary-layer measurements were made on a solid flat plate to provide a basis for comparison of the effectiveness of the various air-injection configurations in reducing skin friction. The boundary-layer velocity profiles measured 12, 14, 16, and 19.325 inches from the leading edge of the solid-plate configuration are presented in figure 6. Good agreement was obtained with the standard 1/7-power turbulent profile as indicated in figure 6(d). With the use of the velocity profiles, the momentum thickness θ was calculated from the relation

$$\theta = \int_0^{\delta} \frac{\rho u}{\rho_\infty U_\infty}\left(1 - \frac{u}{U_\infty}\right)dy$$

The integrand was plotted against the height above the surface y in figure 7. From a graphical integration of the integrand profiles, values of θ were obtained and are plotted against distance along the plate in figure 8.

Inasmuch as transition to turbulent flow was attained through the use of a boundary-layer trip near the model leading edge, it was necessary to determine the position of the virtual origin of the turbulent boundary layer. The momentum thicknesses presented in figure 8 were used with the method of reference 9 to determine the virtual origin which was calculated to be located 0.63 inch forward of the leading edge. The distance from the virtual origin to the position of any measurement was used as the reference length, and the product of the span of 14 inches and the reference length was used as the reference area for the air-injection results.

The average and local skin-friction coefficients measured on the solid plate are plotted against distance along the plate in figure 9. The average skin-friction coefficient was determined from the relation $C_{F,o} = \frac{2\theta}{x_v}$ since θ for the solid plate includes skin friction only and x_v is the distance between the virtual origin and the measuring station. The values of local skin-friction coefficient presented were obtained from the variation of θ with x (fig. 8) with the relation $C_{f,o} = 2\frac{d\theta}{dx_v}$. At the 19.327-inch station (the location of the boundary-layer survey), the value of $C_{f,o}$ was 1.401×10^{-3}. This value compares favorably with a $C_{f,o}$ of 1.39×10^{-3} obtained from the skin-friction balance at the 20-inch station.

Air Injection

Distributed.- Results obtained with a distributed injection of air into the boundary layer through a porous surface are presented in figure 10. The ratio of the average or local skin-friction coefficient measured near the rear of the model with injection to the value measured on the solid plate without injection $\frac{C_F}{C_{F,o}}$ or $\frac{C_f}{C_{f,o}}$ is plotted against the mass-flow parameter $\frac{2F}{C_{F,o}}$. Both the average and local skin-friction coefficient decreased with increasing flow rate reaching a maximum reduction of approximately 20 percent, at the maximum test flow rate. It must be noted that at the local skin-friction balance position, the boundary layer is in transition from the porous surface to the solid surface with a consequent change in wall shear force for the porous injection cases. The reduction in average skin friction is in good agreement with the results obtained in reference 5 for porous injection on a cone model. The velocity profiles at the 19.325-inch station are presented in a dimensional and a nondimensional form in figures 11 and 12, respectively. Not only did distributed injection thicken the boundary layer, which would decrease the local skin friction in a boundary layer that conformed to the normal nondimensional turbulent profile, but distributed injection also distorted the nondimensional velocity profiles in a manner which further reduced the velocity slope at the wall with an additional favorable effect on skin friction.

Flush slots.- The variation of average skin-friction-coefficient ratio with mass-injection rate is presented in figure 13 for the four flush slots having different widths. Except for the narrowest slot tested (w = 0.018 inch), an increase in average skin friction was measured with injection, with the adverse effect increasing with increased slot width. The reduction in $\frac{C_F}{C_{F,o}}$ obtained with the 0.018-inch-wide slot reached a maximum of 10 to 15 percent at a value of $\frac{2F}{C_{F,o}}$ of 0.45 and remained fairly constant with further increases in injection rate.

The local skin friction at the 20-inch station decreased with increasing injection rate for all slot widths (fig. 14), a trend consistent with most of the changes in the boundary-layer velocity profiles at the same station (fig. 15). The observed increase in average skin friction near the 19.325-inch station, when the local skin friction at that station was decreased, indicates an adverse effect of the injected air on the boundary-layer profiles at some position forward of the measuring station and an associated increase in the local skin frictions at the forward positions. The nature of this adverse mixing effect can be determined only through additional boundary-layer surveys in the mixing region although the present results appear to indicate smaller adverse mixing effects with the narrower slots.

Step slot.- The average and local skin-friction coefficients at the rearmost stations, as fractions of the solid-plate coefficients, are presented in figure 16 for the 0.068-inch-wide rearward-inclined step slot. The results for the 0.065-inch-wide flush slot are also given for comparison. With no air injection through the step slot, the average skin-friction coefficient was approximately 85 percent of that on the solid plate, probably because of separation of the flow downstream of the rearward-facing step. Although the local skin friction equaled the solid-plate value at the 20-inch station (fig. 16(b)), it is likely that lower local values in the separated region resulted in the lower average at the rearmost station.

Injection of air through the step slot increased the average skin friction to the point that almost no reduction was attained at the maximum test flow rate. Even at the rearmost station, the local skin-friction coefficients were greater than the values for the solid plate through the test range of injection flow rate. The trend of the measured local skin-friction coefficient with injection flow is in agreement with the velocity gradient in the boundary layer near the surface at about the measuring point in the boundary layer closest to the surface, which was maintained at a constant height of 0.0035 inch (fig. 17). It appears, then, that even though the boundary layer was thickened, injection through the step slot increased the local skin-friction coefficients because of increased velocities near the surface. This undesirable distortion or change in the power of the velocity profile, as contrasted with the favorable distortion obtained with distributed injection (fig. 12), can be seen in figure 18, where the nondimensional profiles for the step slot are compared with the 1/7-power profile.

Other considerations.- Although distributed injection produced the greatest decrease in skin friction, this does not necessarily mean that it has the

greatest overall effectiveness in reducing drag. If distributed injection is used, the total momentum of the air used for injection is lost. When the air is injected through rearward-inclined slots, however, most of the momentum of the air is recovered and a greater overall drag reduction might be obtained. Whether or not this is the case depends on the momentum of the air available for injection, and a close examination of each individual situation is required before a definite conclusion can be reached.

CONCLUDING REMARKS

A preliminary investigation has been made at a Mach number of 3 of the effectiveness of injection of air into the boundary layer through a porous surface and through single rearward-inclined slots in reducing the level of supersonic turbulent skin friction. A reduction in the average turbulent skin-friction coefficient of approximately 20 percent was obtained by distributed air injection through a porous surface. The most effective slot configuration investigated was the narrowest flush slot (0.018 inch wide), which provided a reduction in average skin-friction coefficient of 10 to 15 percent. All other slots tested resulted in an increase in skin friction with increased injection rate. Although the distributed air injection resulted in a greater decrease in skin friction than the rearward-inclined slots, other considerations such as momentum recovery of the injection air must be considered before a conclusion can be made as to which type of injection is the most effective in reducing overall drag. The effectiveness of the various slot configurations in reducing skin friction appears to be largely dependent on the manner in which the injected air mixes with the original boundary layer. Additional boundary-layer surveys in closer proximity to the slots are required to evaluate more completely the mixing effects and to assist in the development of more effective configurations.

Langley Research Center,
National Aeronautics and Space Administration,
Langley Station, Hampton, Va., May 7, 1964.

REFERENCES

1. Dorrance, William H., and Dore, Frank J.: The Effect of Mass Transfer on the Compressible Turbulent Boundary-Layer Skin Friction and Heat Transfer. Jour. Aero. Sci., vol. 21, no. 6, June 1954, pp. 404-410.

2. Rubesin, Morris W.: An Analytical Estimation of the Effect of Transpiration Cooling on the Heat-Transfer and Skin-Friction Characteristics of a Compressible, Turbulent Boundary Layer. NACA TN 3341, 1954.

3. Rubesin, Morris W., Pappas, Constantine C., and Okuno, Arthur F.: The Effect of Fluid Injection on the Compressible Turbulent Boundary Layer - Preliminary Tests on Transpiration Cooling of a Flat Plate at M = 2.7 With Air as the Injected Gas. NACA RM A55I19, 1955.

4. Rubesin, Morris W., and Pappas, Constantine C.: An Analysis of the Turbulent Boundary-Layer Characteristics on a Flat Plate With Distributed Light-Gas Injection. NACA TN 4149, 1958.

5. Tendeland, Thorval, and Okuno, Arthur F.: The Effect of Fluid Injection on the Compressible Turbulent Boundary Layer - The Effect on Skin Friction of Air Injected Into the Boundary Layer of a Cone at M = 2.7. NACA RM A56D05, 1956.

6. Braslow, Albert L., and Knox, Eugene C.: Simplified Method for Determination of Critical Height of Distributed Roughness Particles for Boundary-Layer Transition at Mach Numbers From 0 to 5. NACA TN 4363, 1958.

7. Shutts, W. H., Hartwig, W. H., and Weiler, J. E.: Final Report on Turbulent Boundary-Layer and Skin-Friction Measurements on a Smooth, Thermally Insulated Flat Plate at Supersonic Speeds. DRL-364, CM-823 (Contract NOrd-9195), Univ. of Texas, Jan. 5, 1955.

8. Hakkinen, Raimo J.: Measurements of Turbulent Skin Friction on a Flat Plate at Transonic Speeds. NACA TN 3486, 1955.

9. Rubesin, Morris W., Maydew, Randall C., and Varga, Steven A.: An Analytical and Experimental Investigation of the Skin Friction of the Turbulent Boundary Layer on a Flat Plate at Supersonic Speeds. NACA TN 2305, 1951.

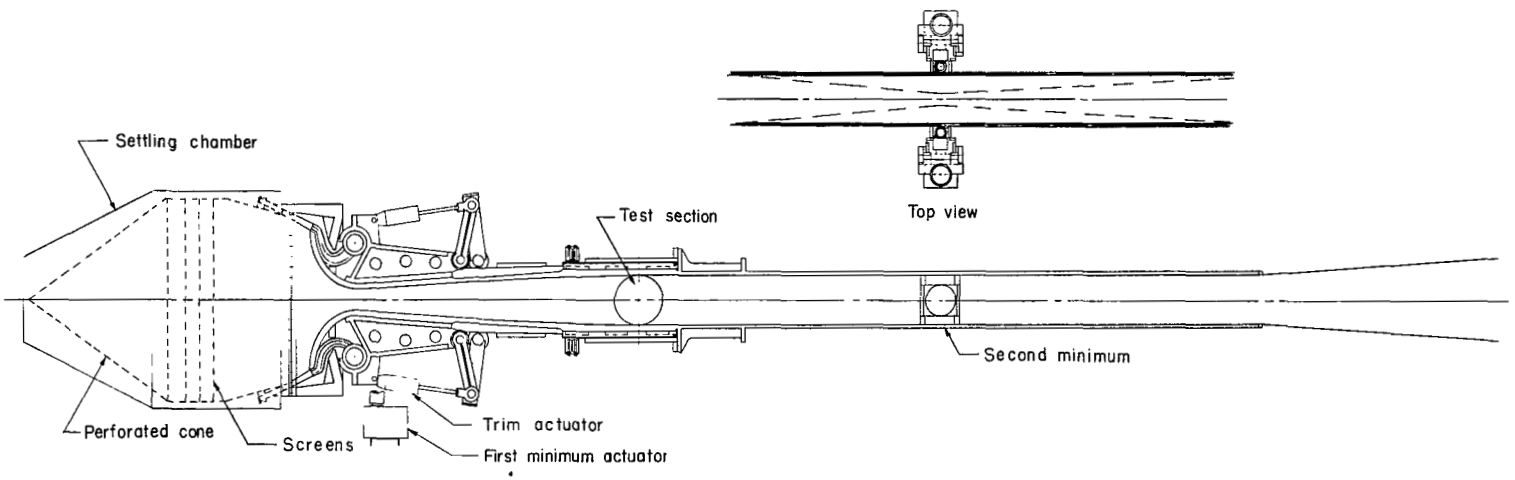

Figure 1.- Schematic drawing of Langley 20-inch variable supersonic tunnel.

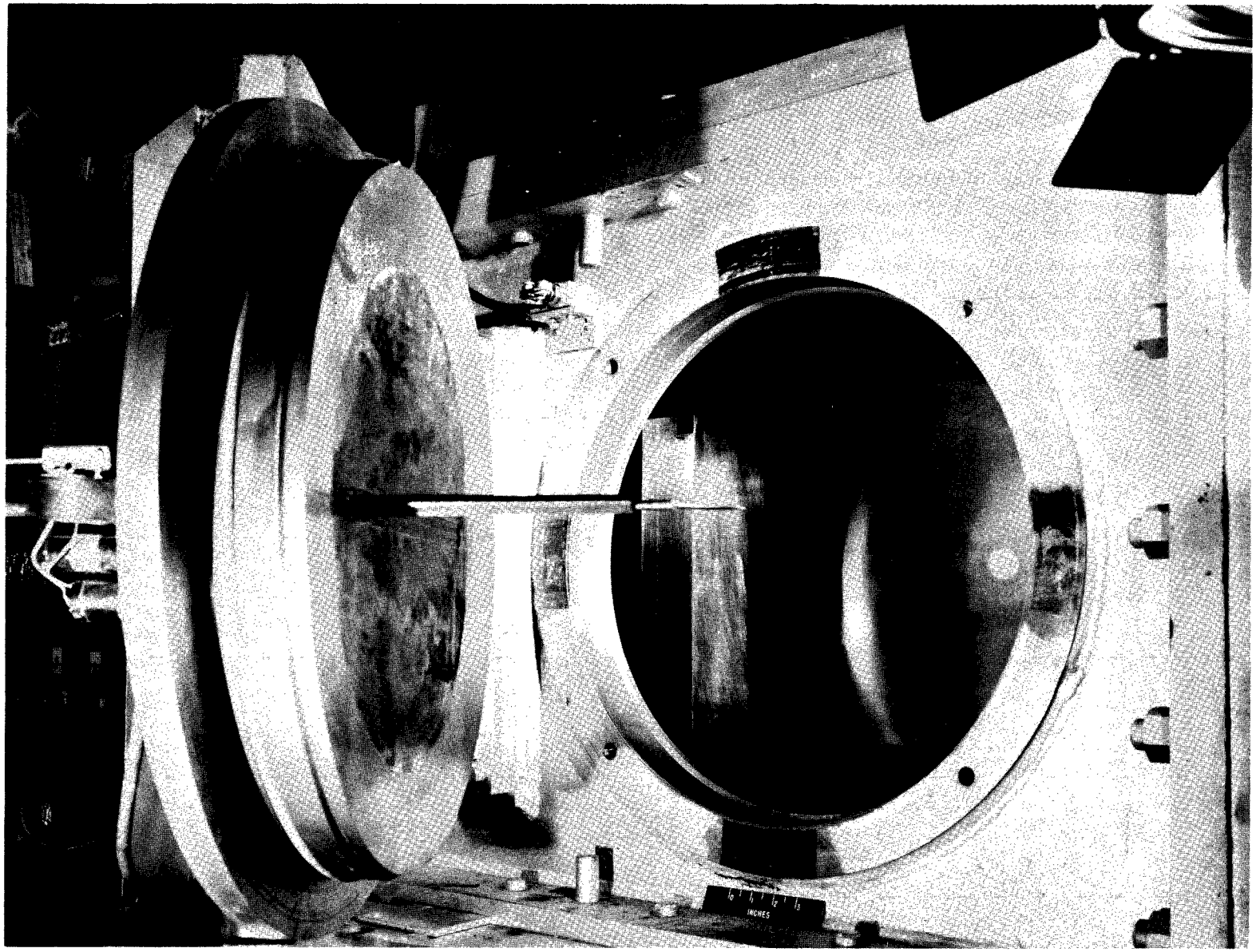

Figure 2.- View of model mounted in the test section with survey probe mounted on the near wall. L-63-800

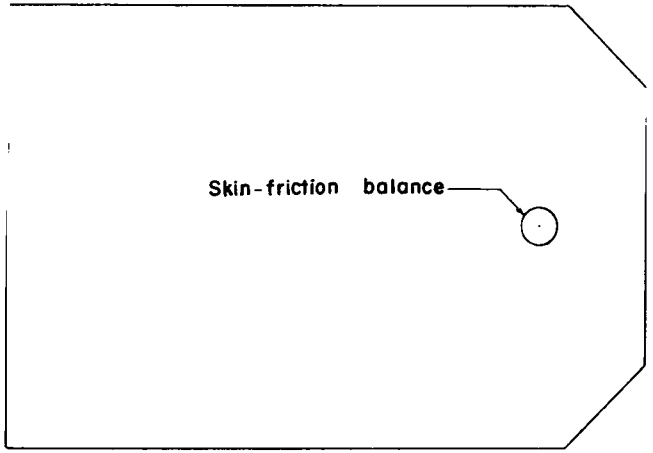

(a) Solid configuration.

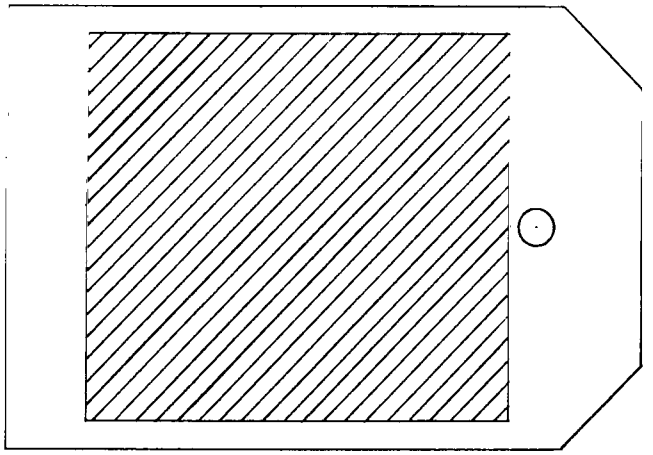

(b) Porous configuration.

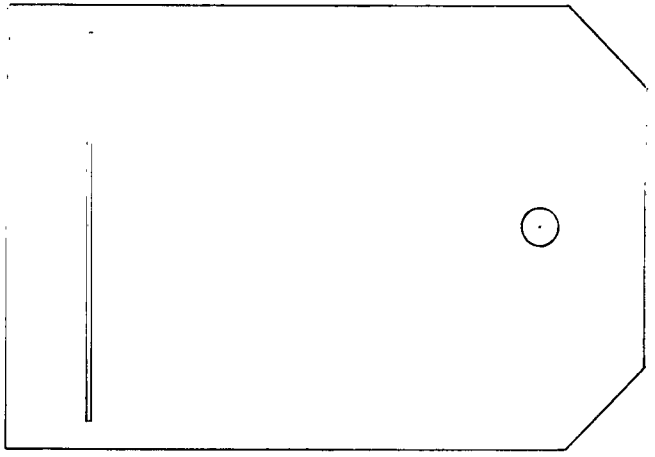

(c) Slot configuration.

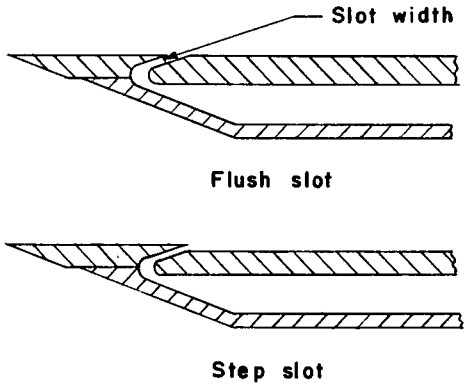

Figure 3.- Sketch of configurations.

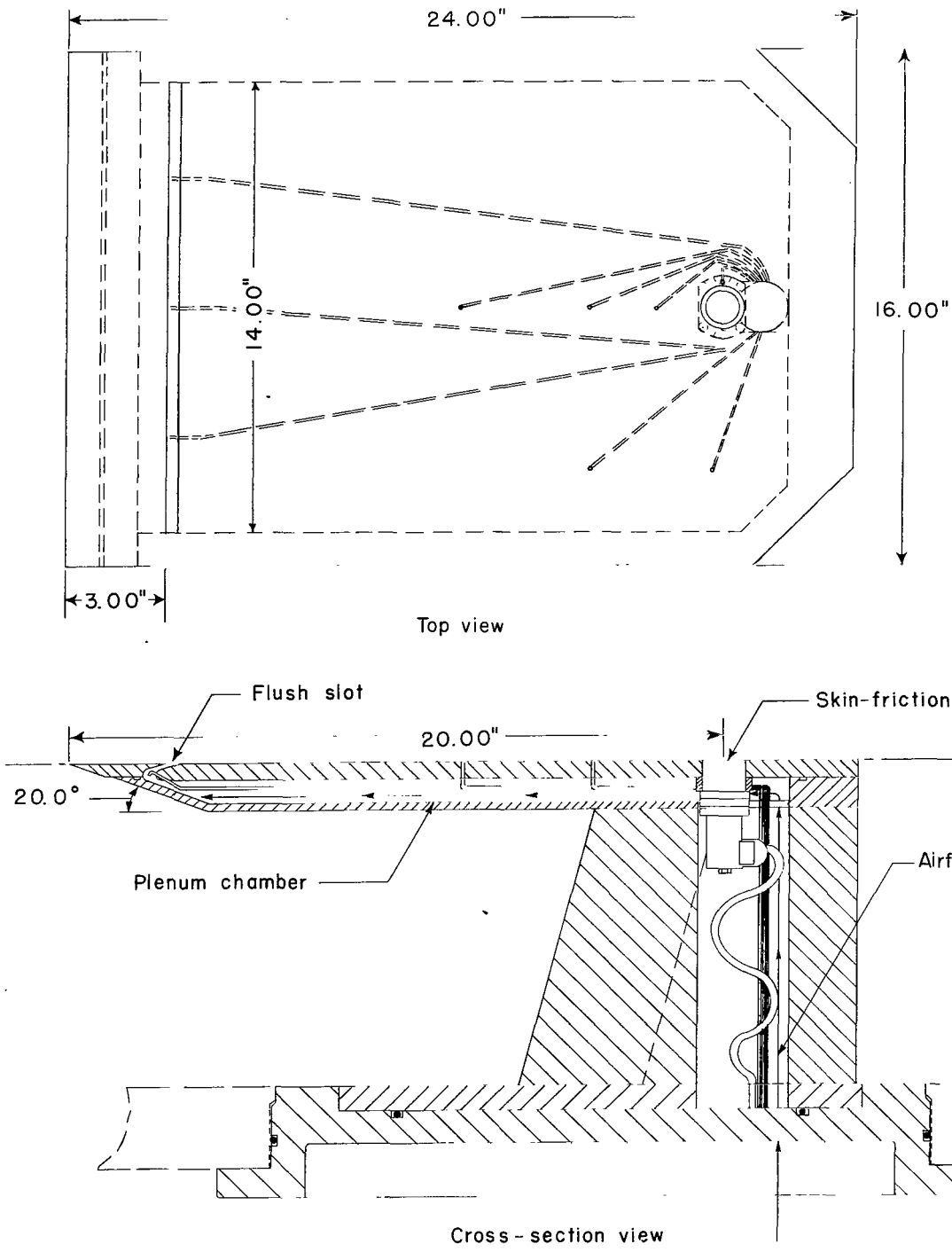

Figure 4.- Sketch of flush-slot air-injection model.

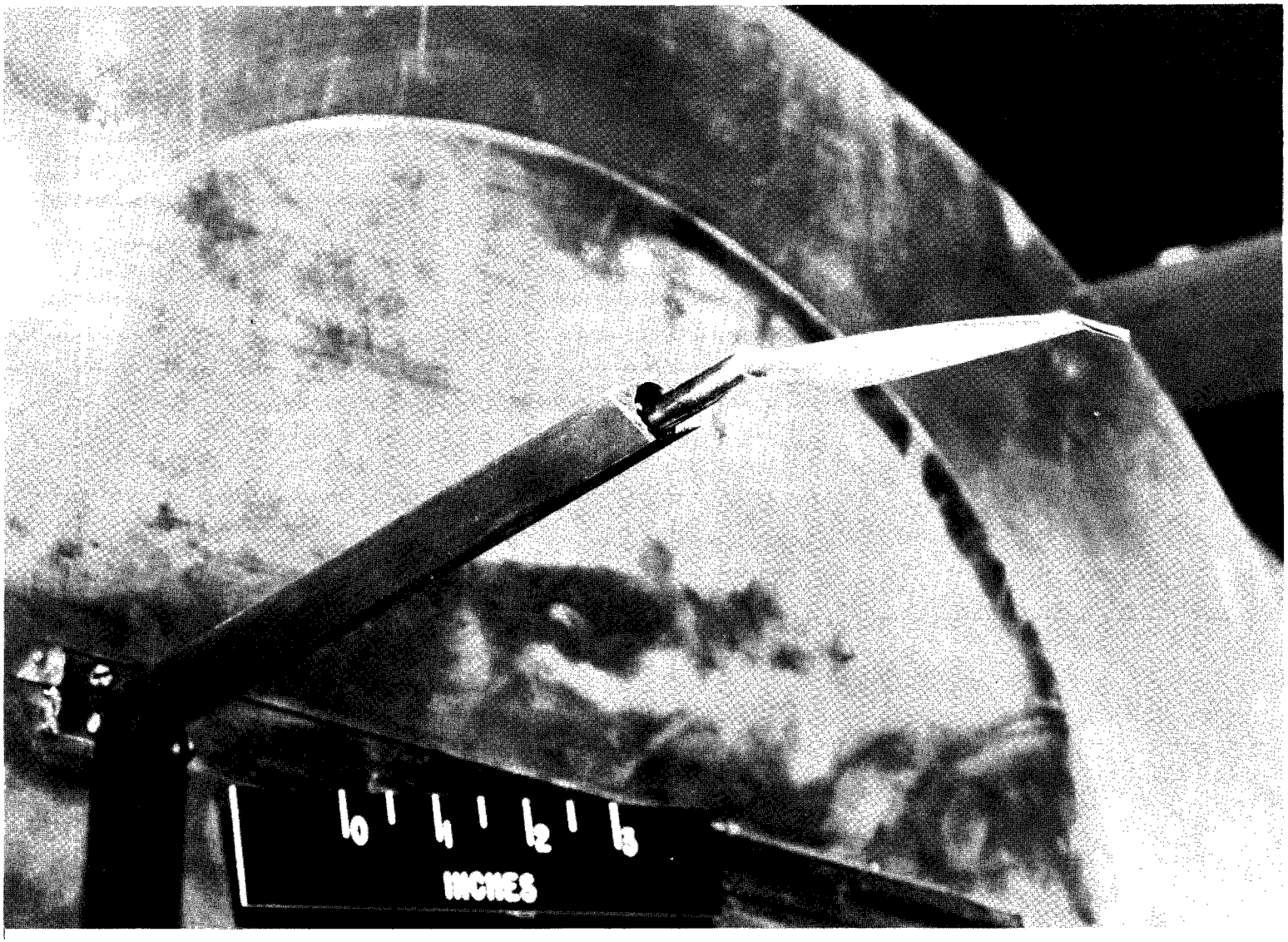

(a) Mounted on tunnel wall.

L-63-797

Figure 5.- Boundary-layer probe.

Front view

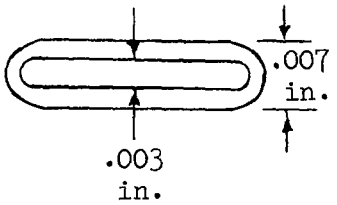

Enlarged view of probe tip

Side view

(b) Schematic of boundary-layer probe with dimensions.

Figure 5.- Concluded.

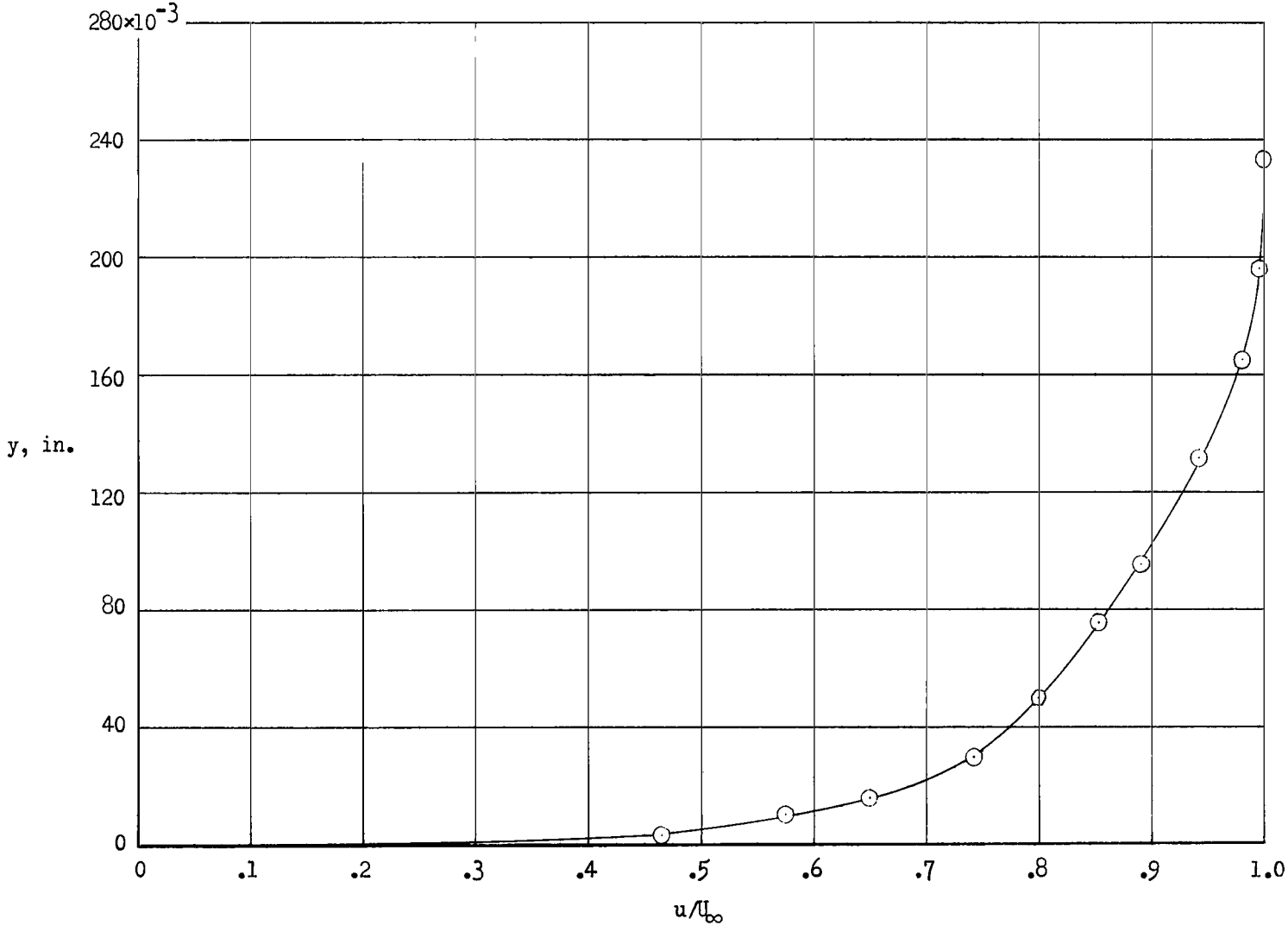

(a) 12 inches from the leading edge.

Figure 6.- Turbulent boundary-layer velocity profiles on the solid-plate configuration.

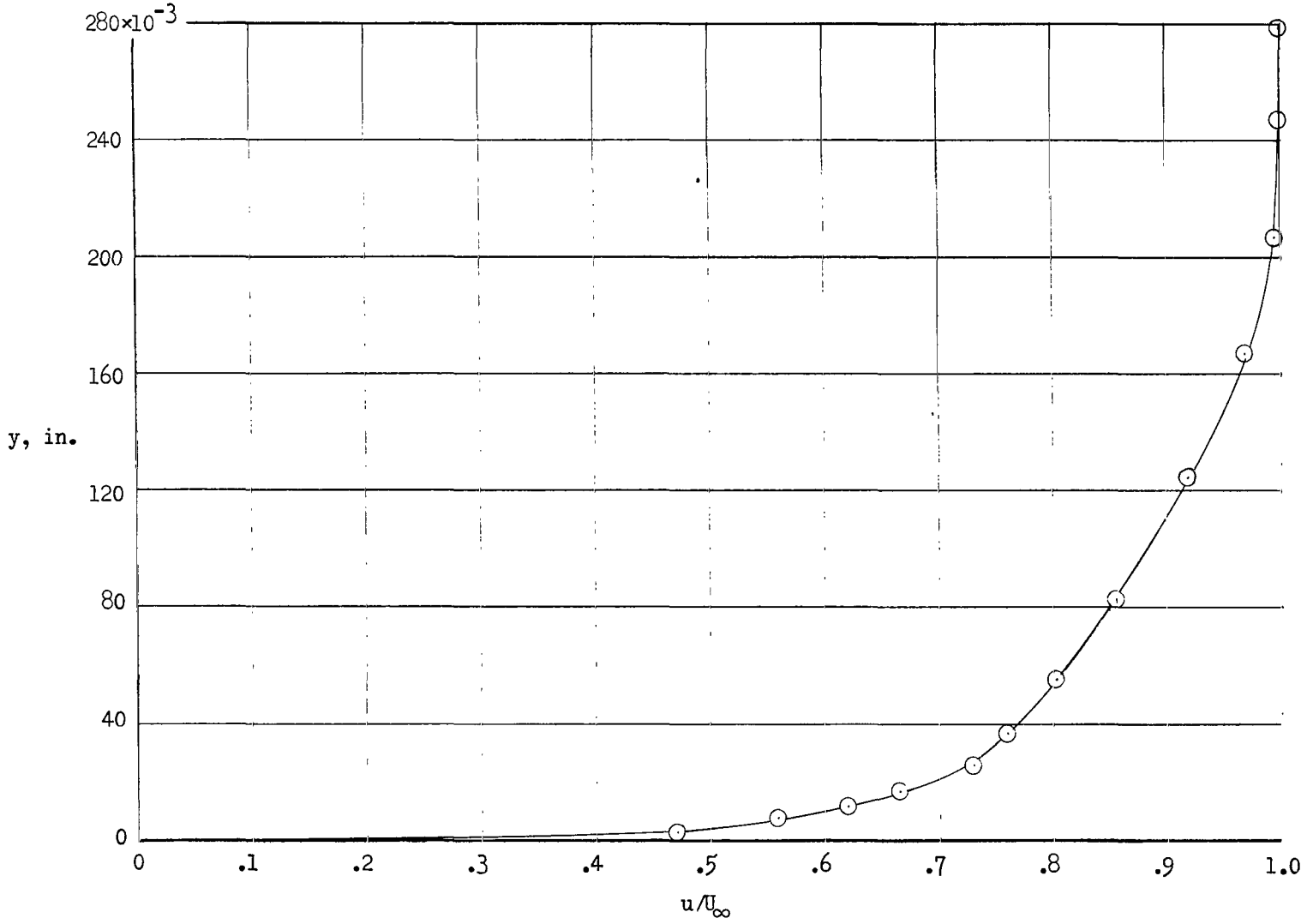

(b) 14 inches from the leading edge.

Figure 6.- Continued.

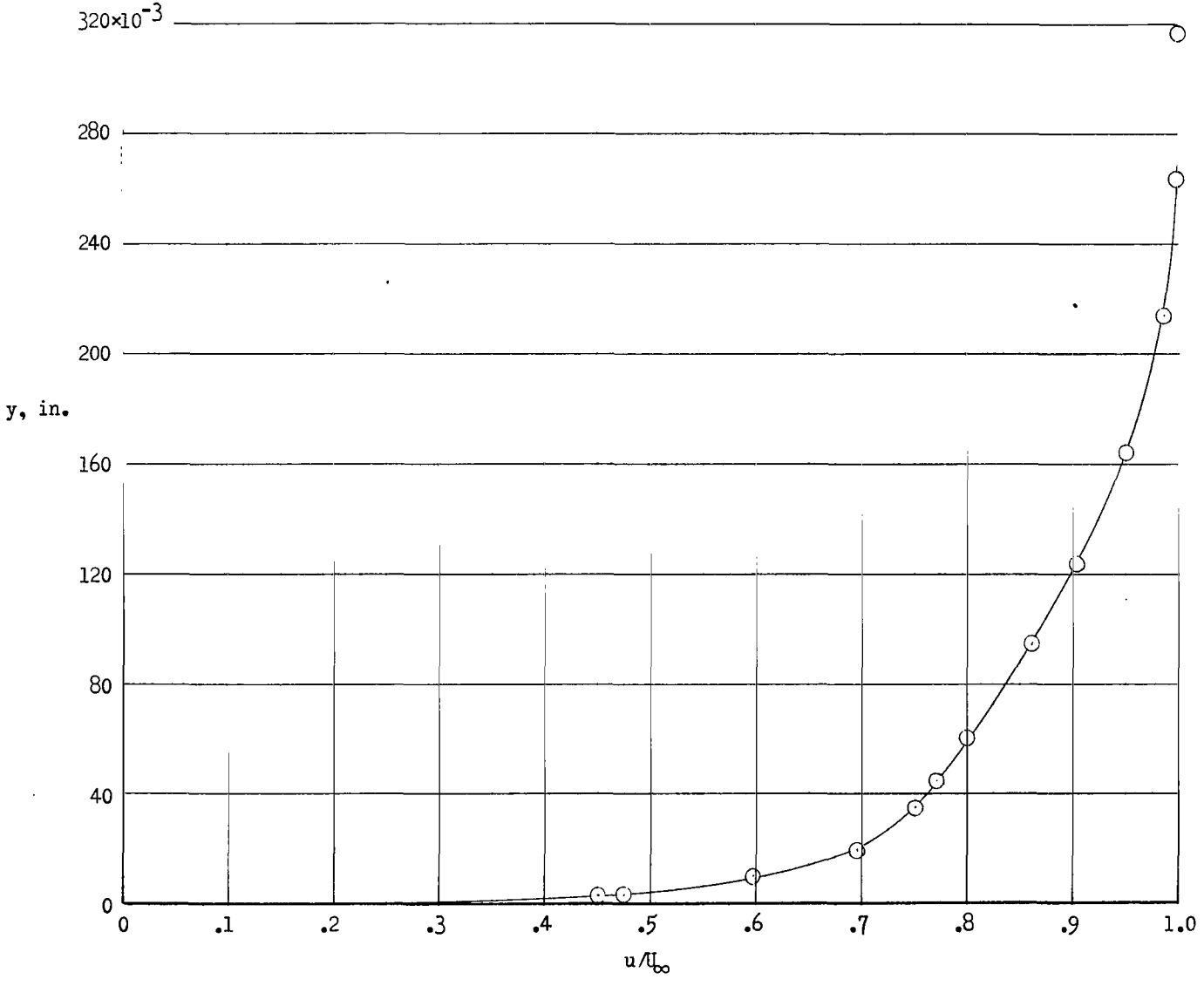

(c) 16 inches from the leading edge.

Figure 6.- Continued.

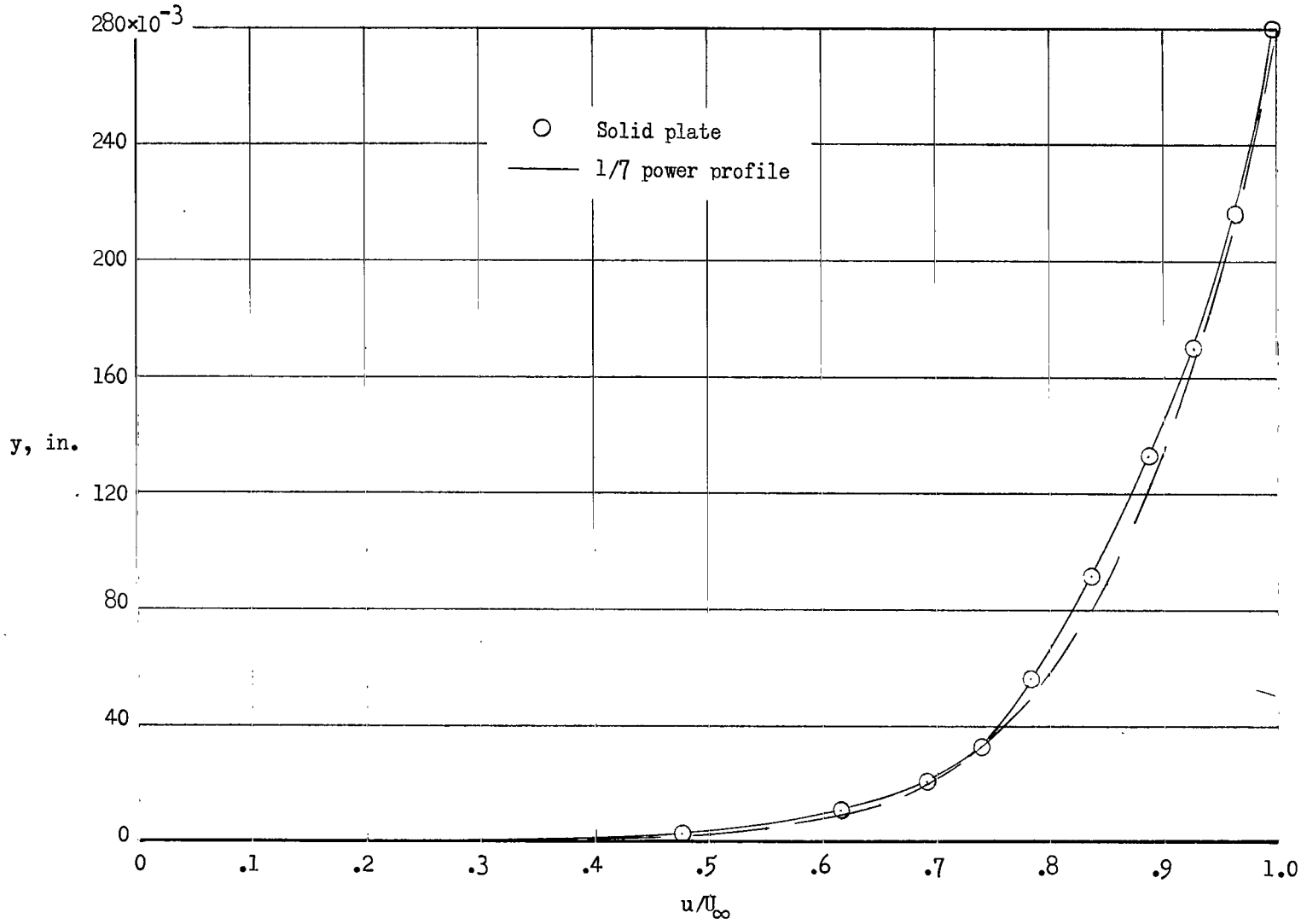

(d) 19.325 inches from the leading edge.

Figure 6.- Concluded.

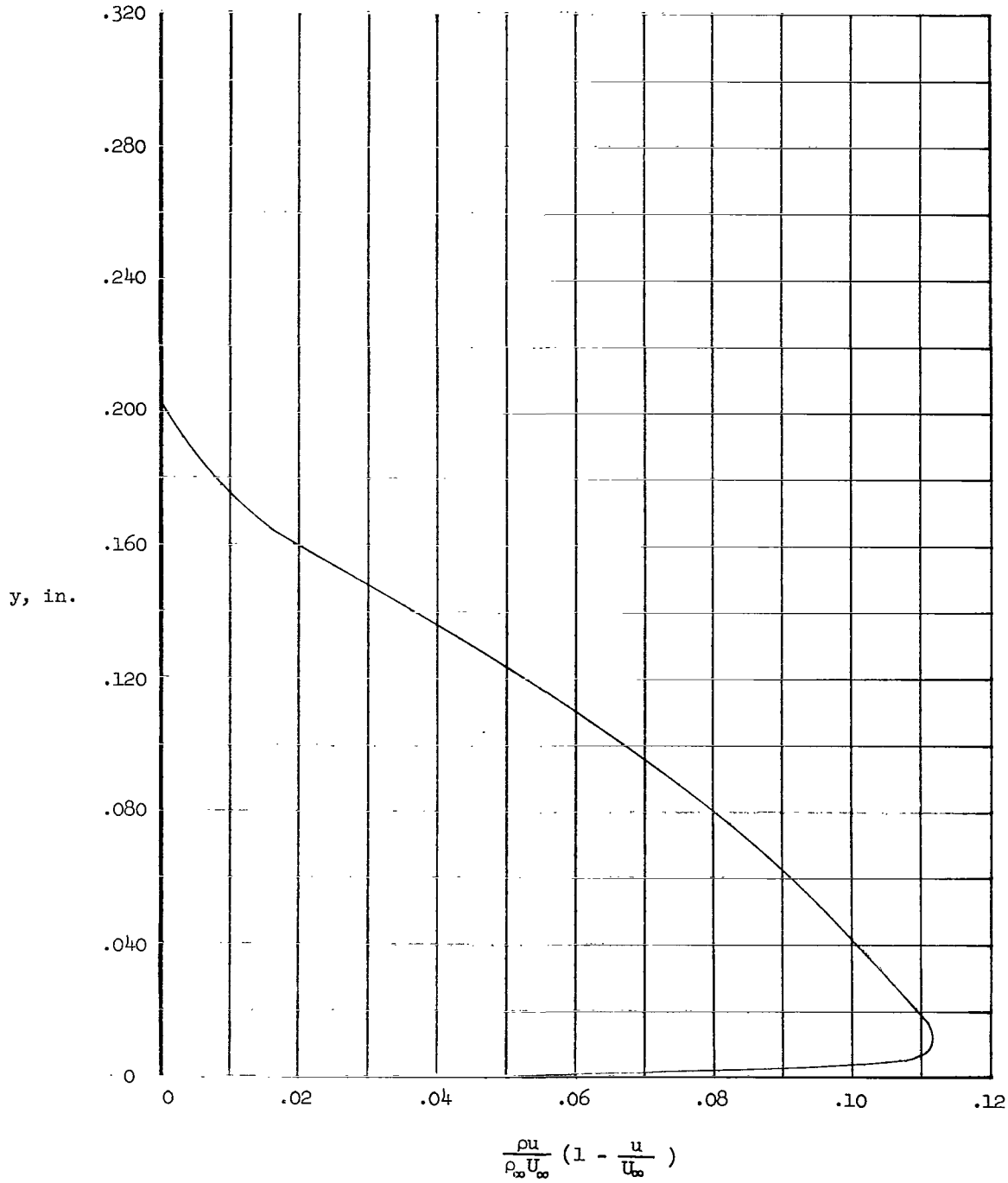

(a) 12 inches from the leading edge.

Figure 7.- Turbulent boundary-layer momentum profiles for the solid plate configuration.

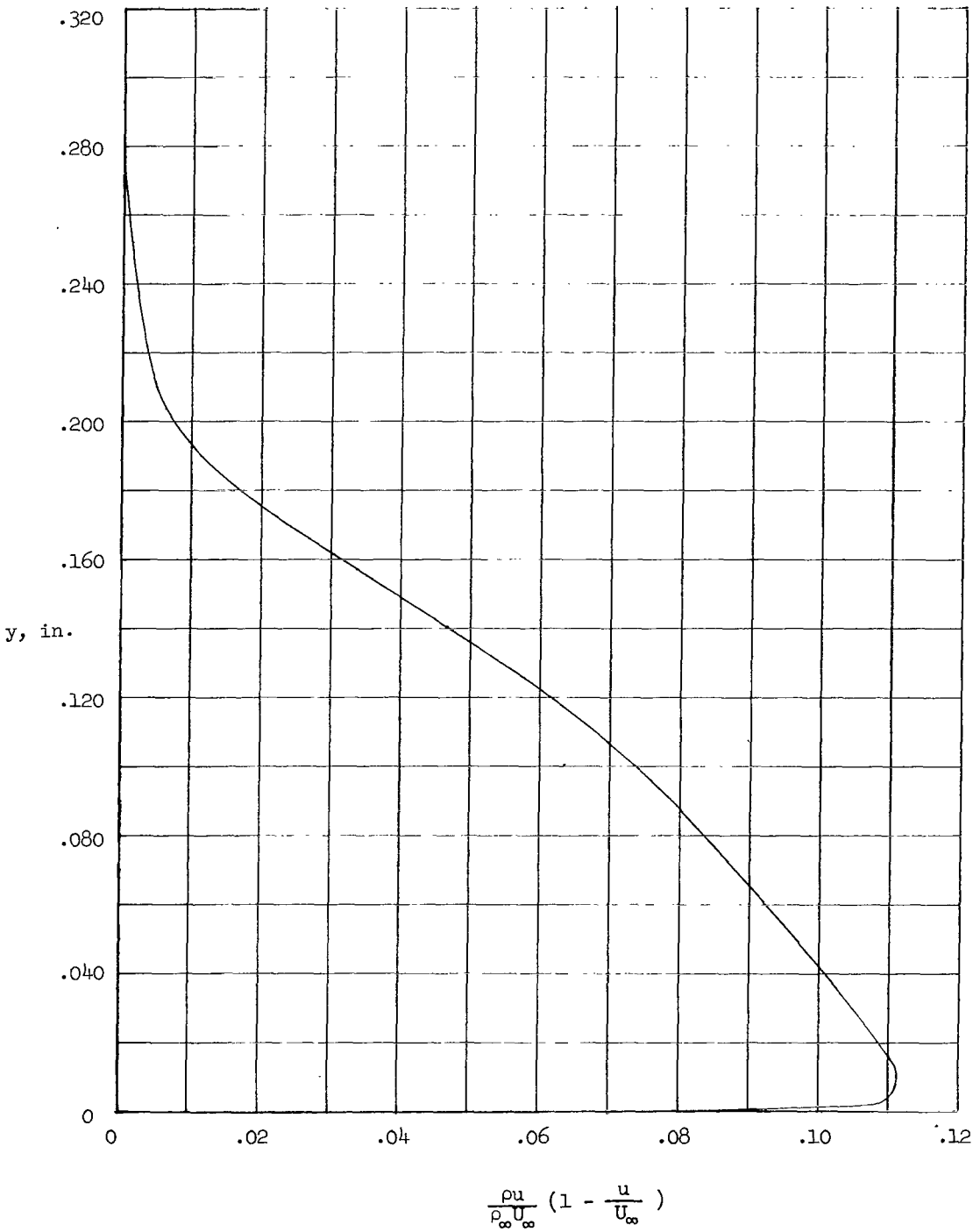

(b) 14 inches from the leading edge.

Figure 7.- Continued.

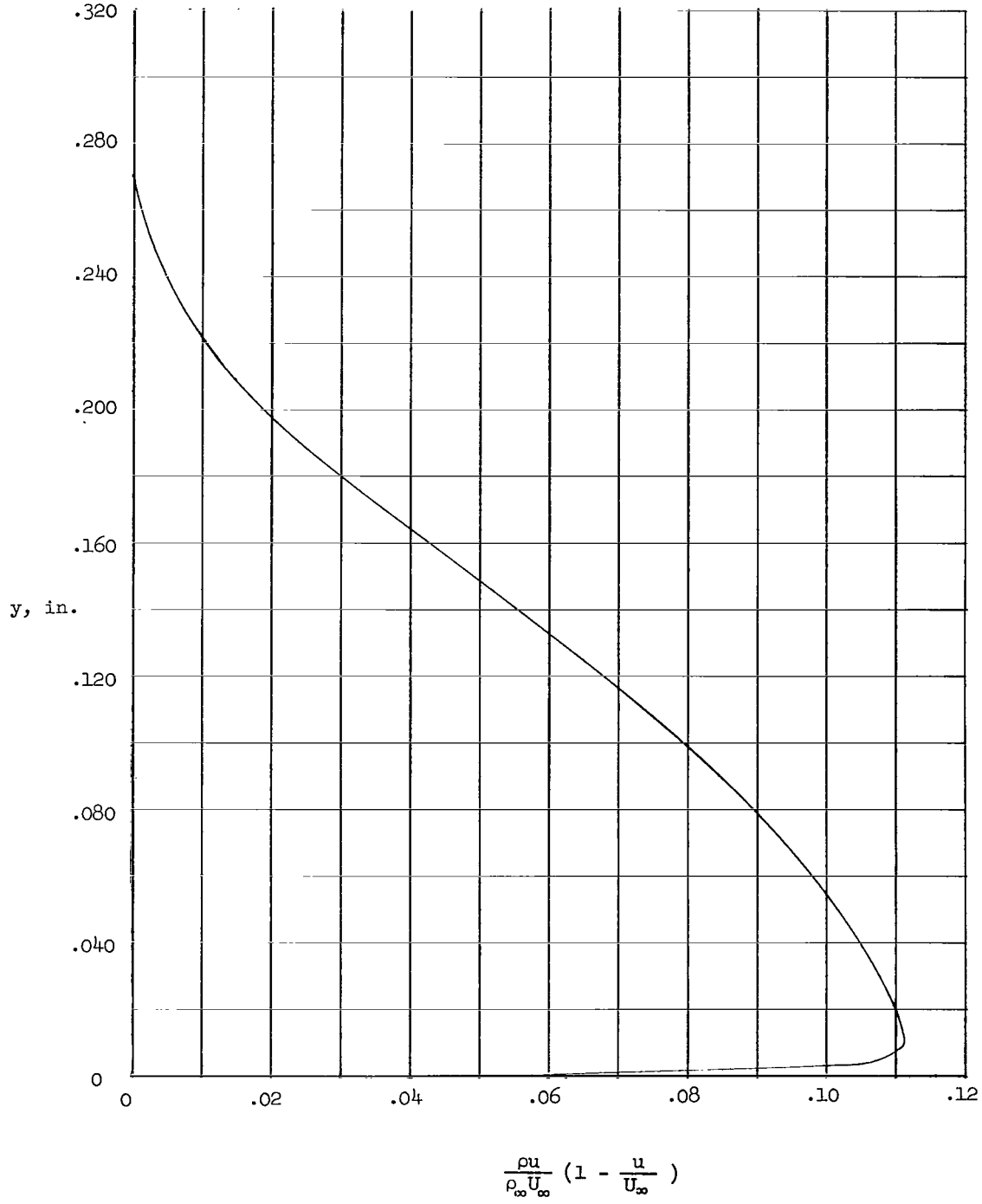

(c) 16 inches from the leading edge.

Figure 7.- Continued.

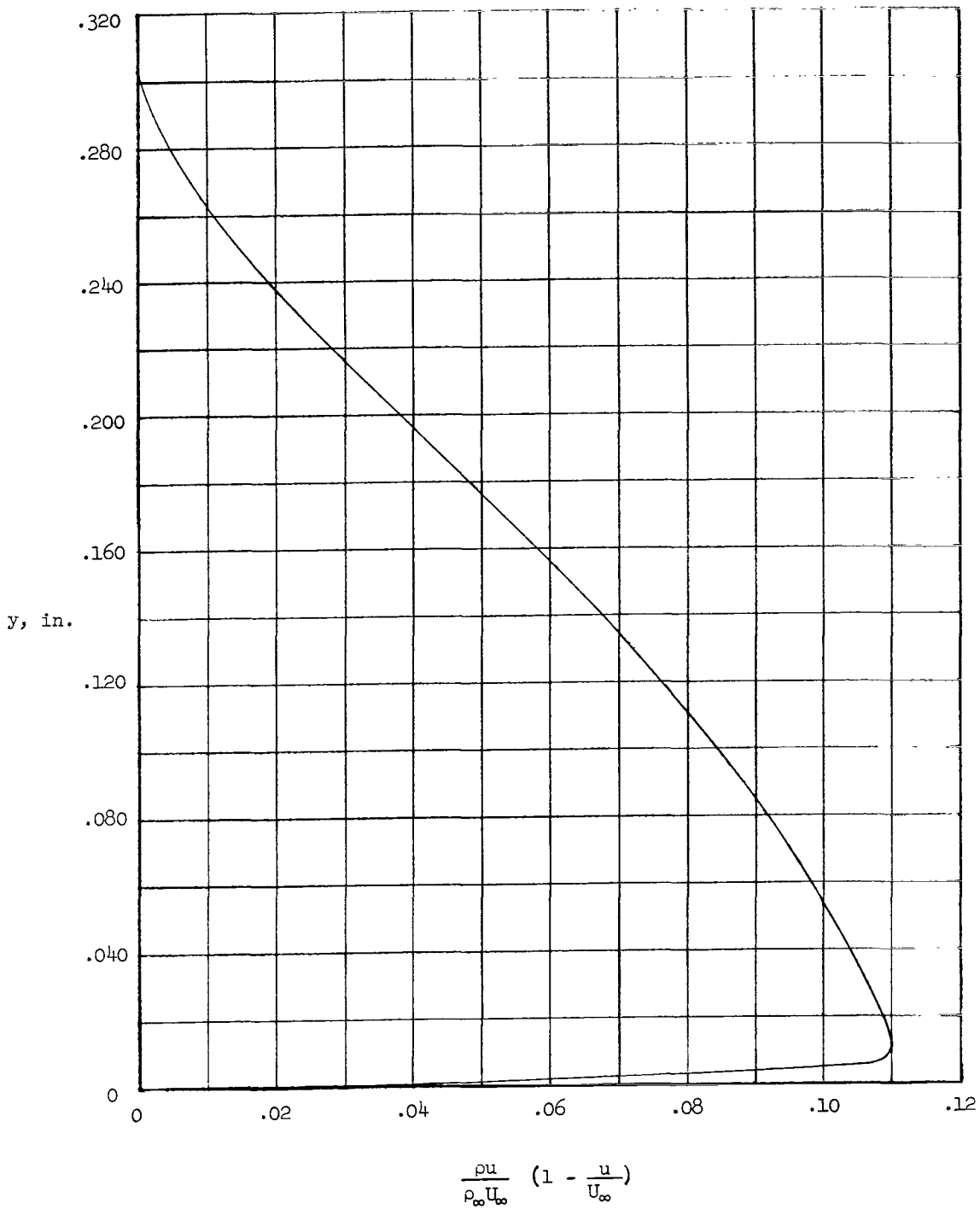

(d) 19.325 inches from the leading edge.

Figure 7.- Concluded.

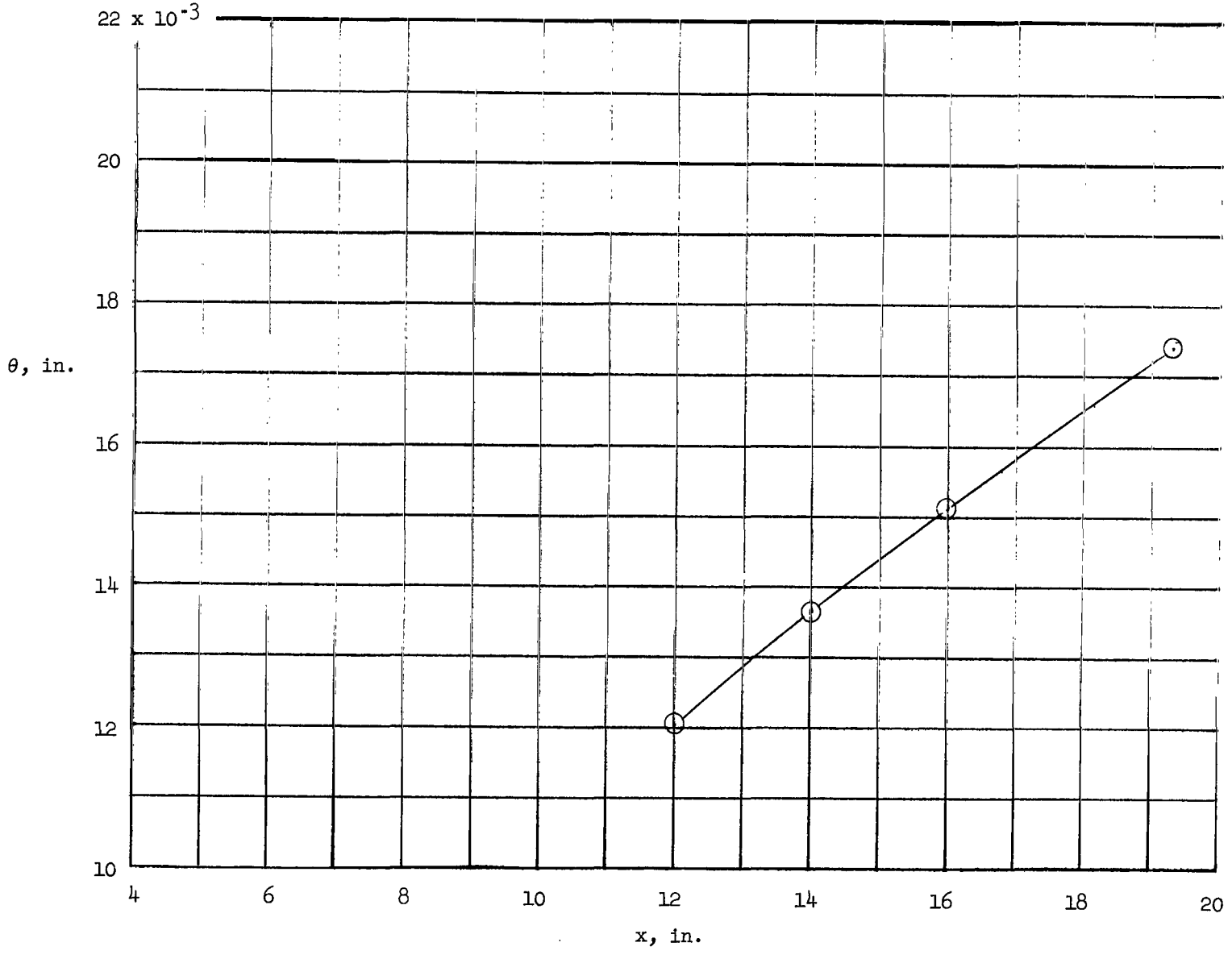

Figure 8.- Momentum thickness with distance from the leading edge for the solid-plate configuration.

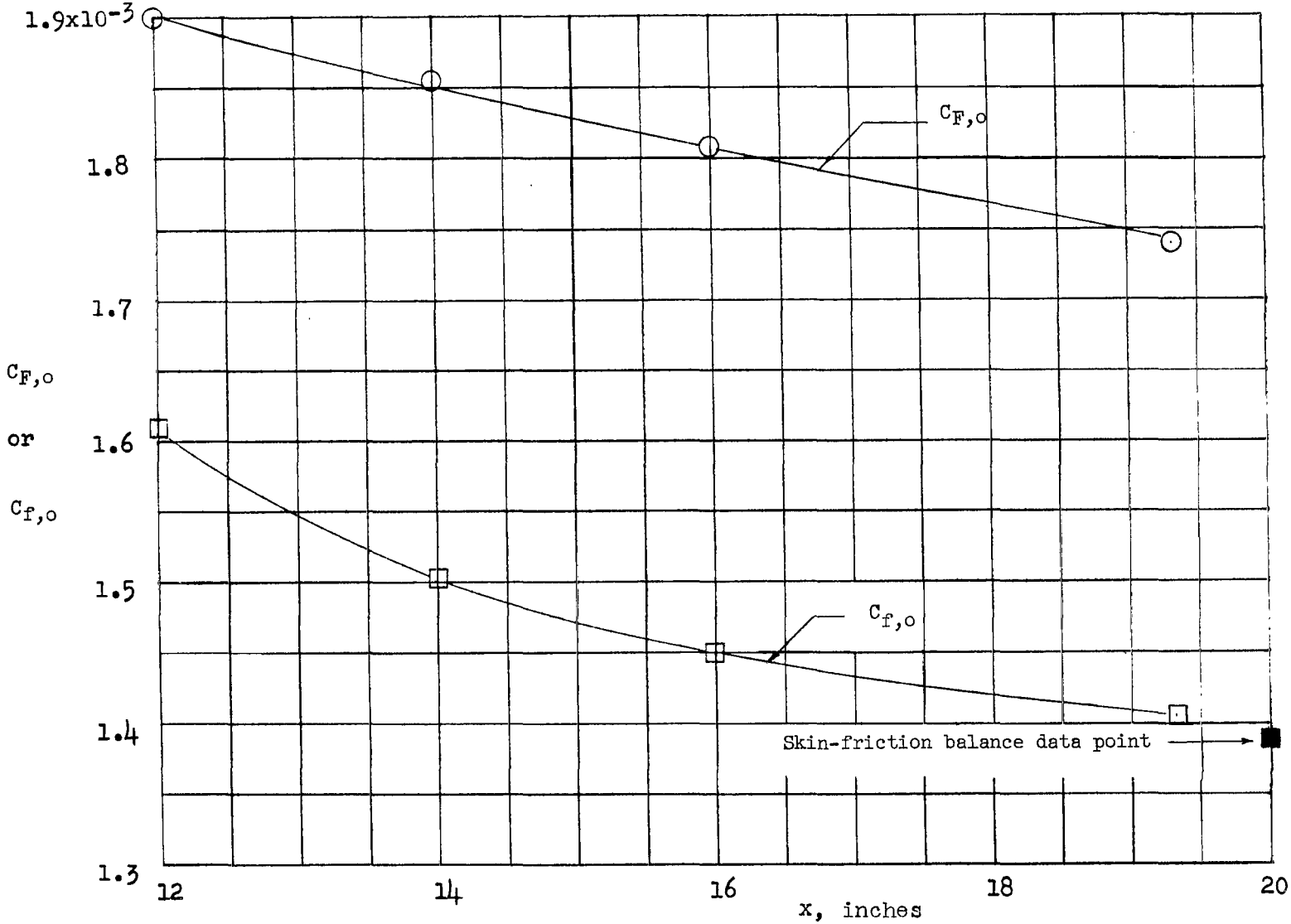

Figure 9.- Average and local turbulent skin-friction coefficients measured on the solid plate.

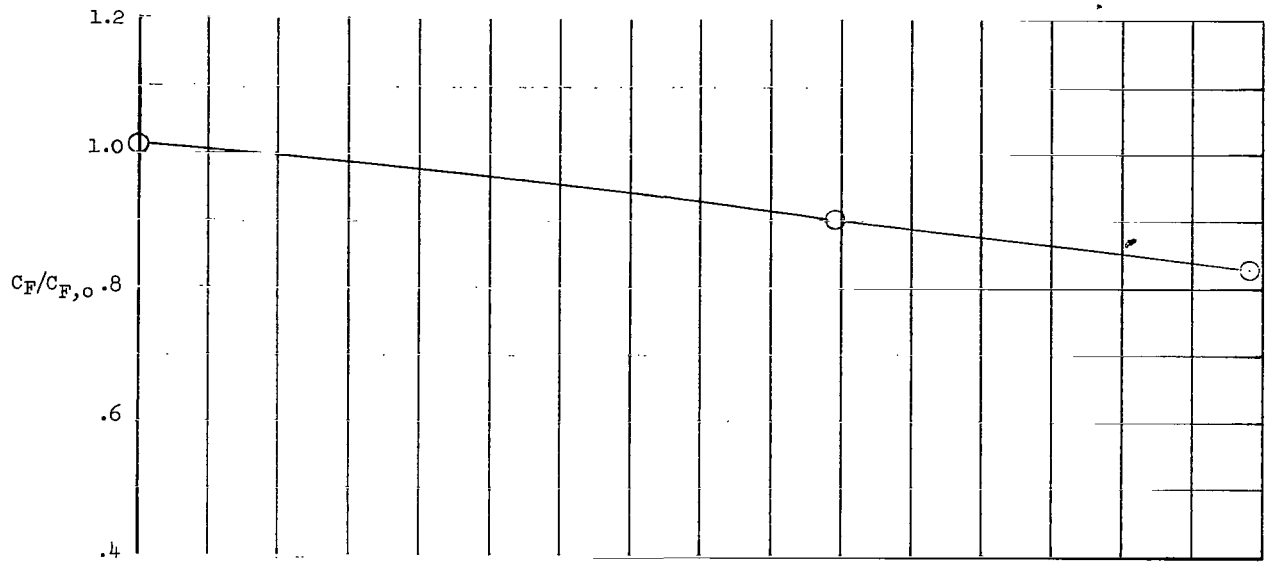

(a) Average skin-friction-coefficient ratio. x = 19.325 inches.

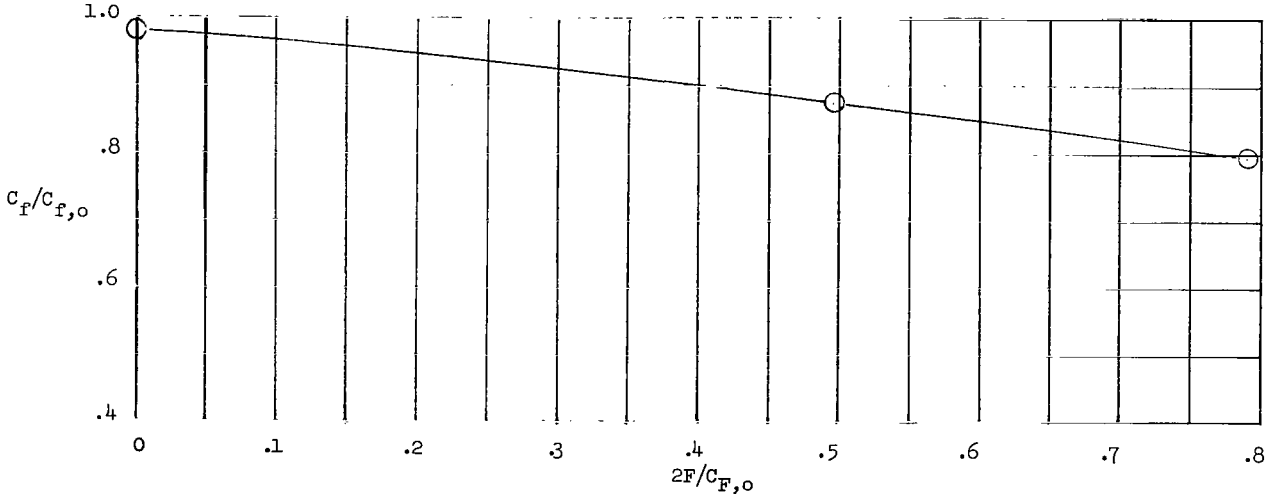

(b) Local skin-friction-coefficient ratio. x = 20 inches.

Figure 10.- Average and local skin-friction-coefficient ratios for porous configuration.

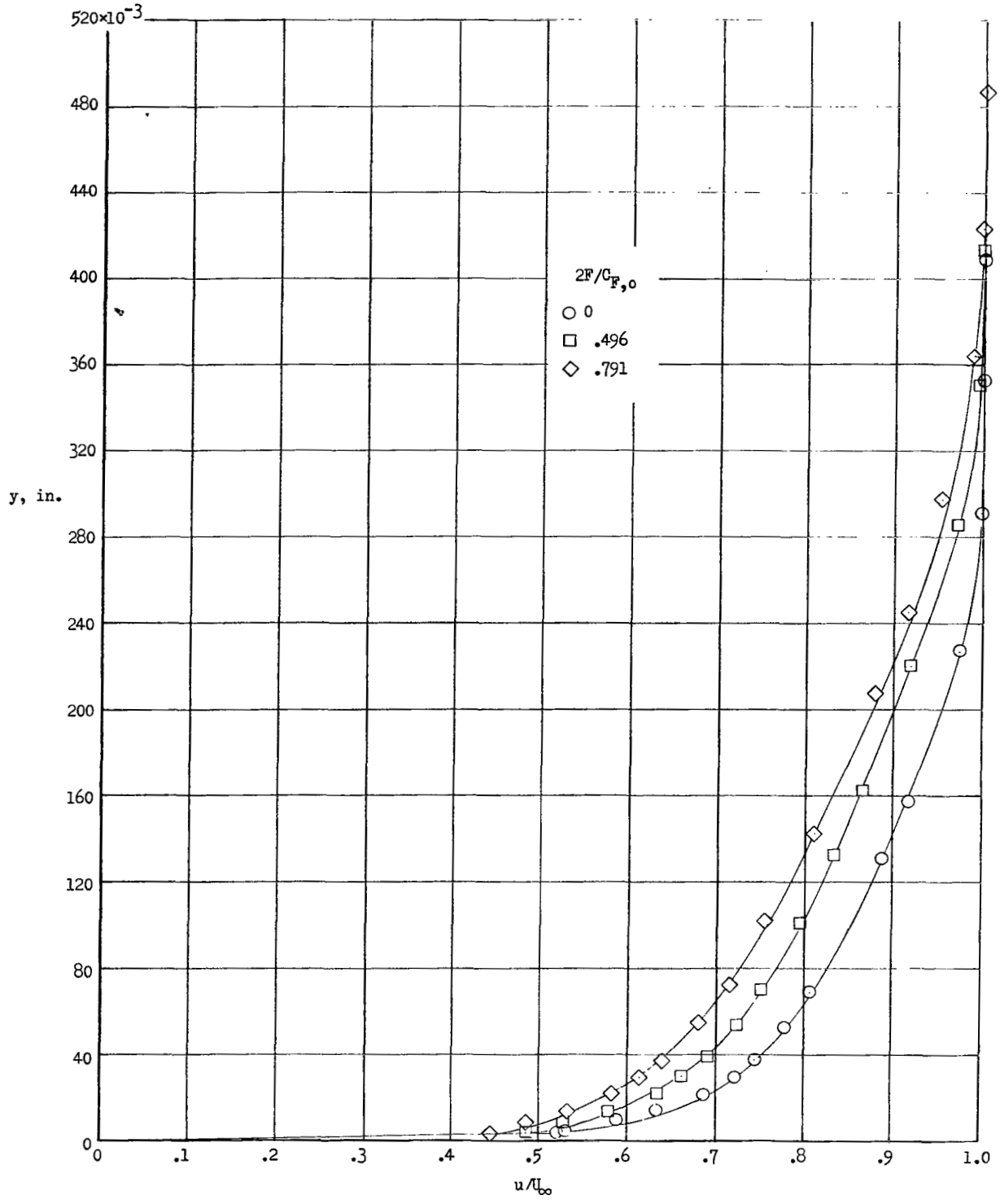

Figure 11.- Velocity profiles for distributed injection. x = 19.325 inches.

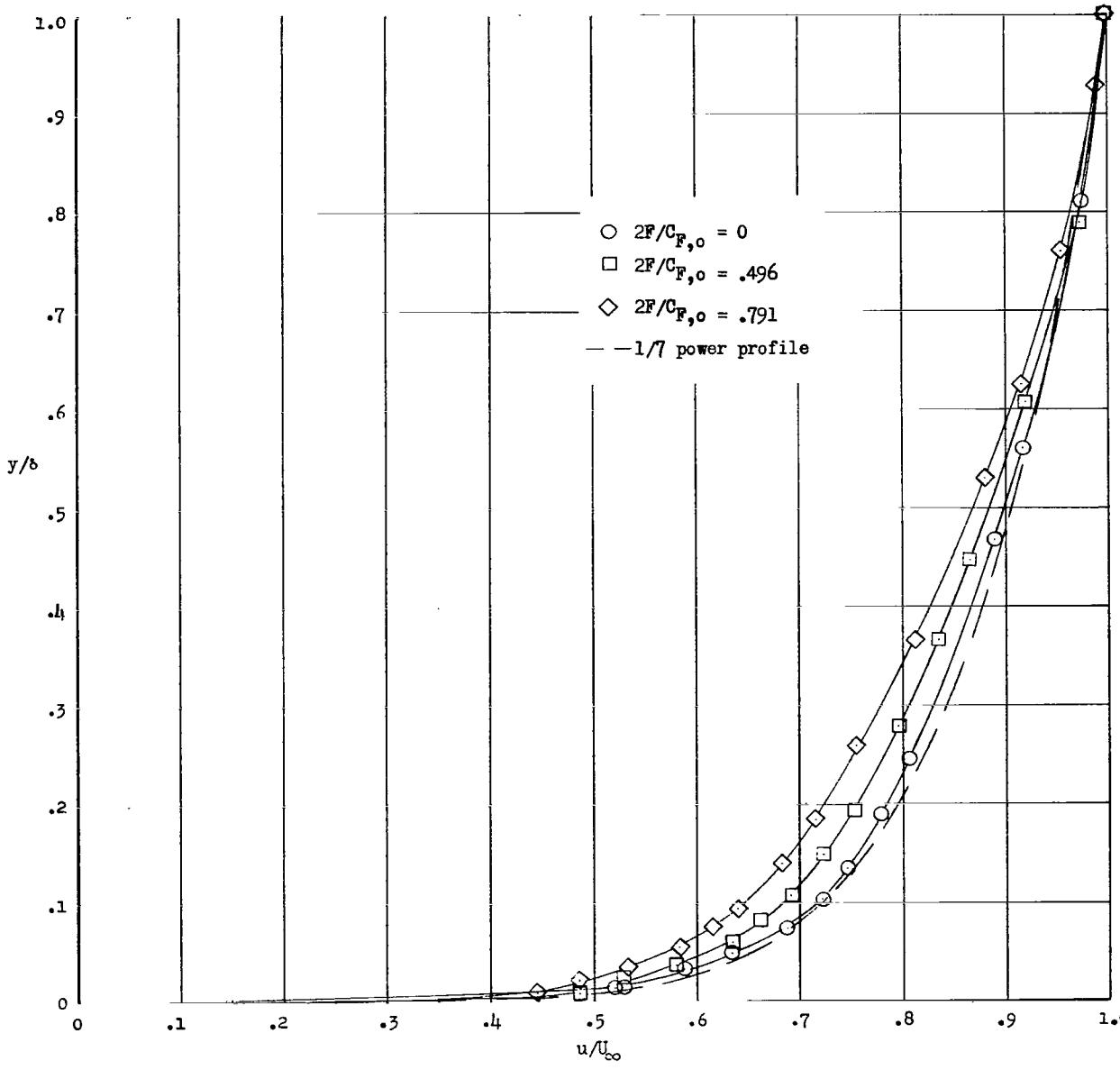

Figure 12.- Comparison between the 1/7-power profile and the velocity profiles for distributed injection. x = 19.325 inches.

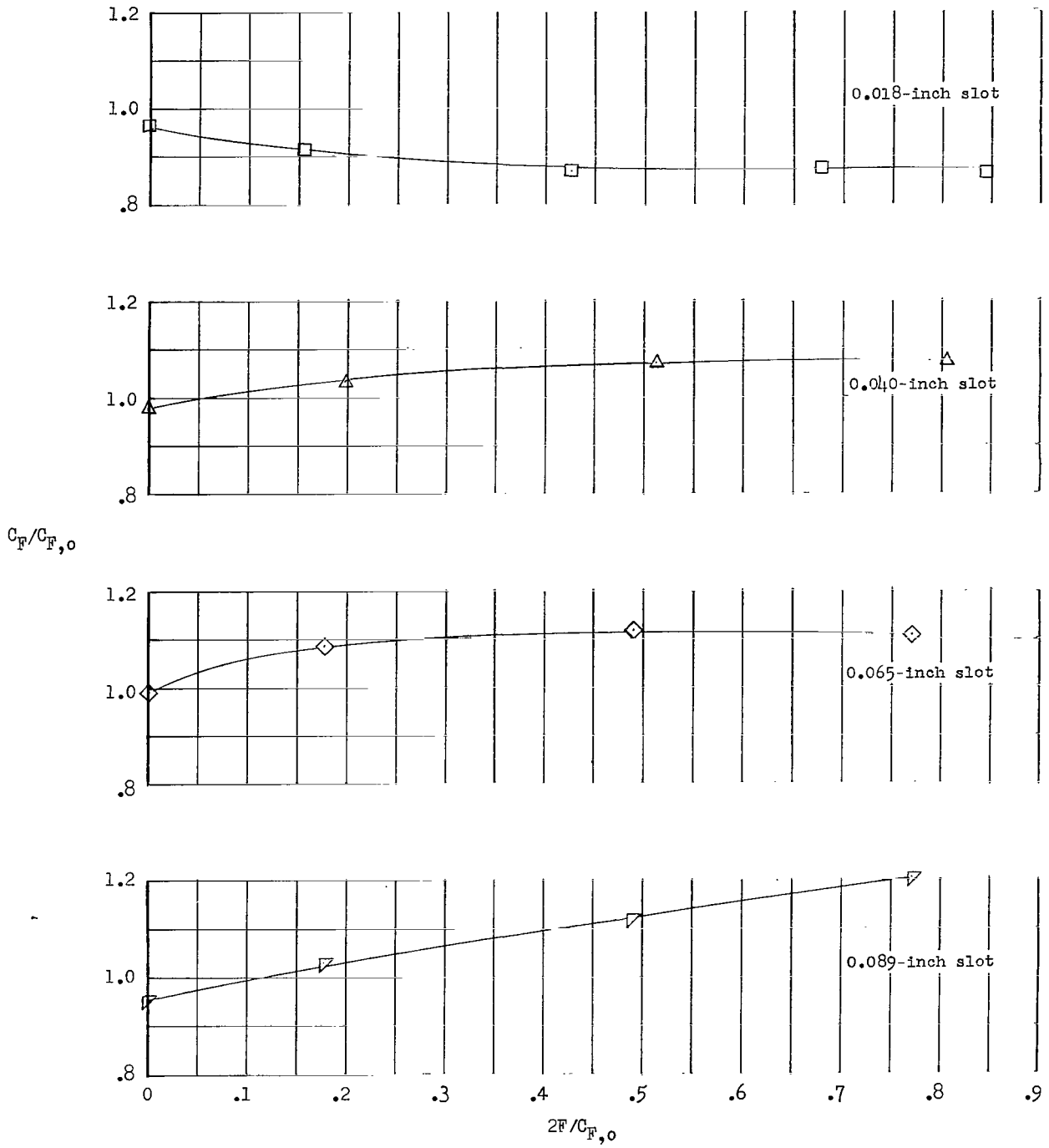

Figure 13.- Average skin-friction-coefficient ratio for different mass-flow rates for the flush-slot configuration. x = 19.325 inches.

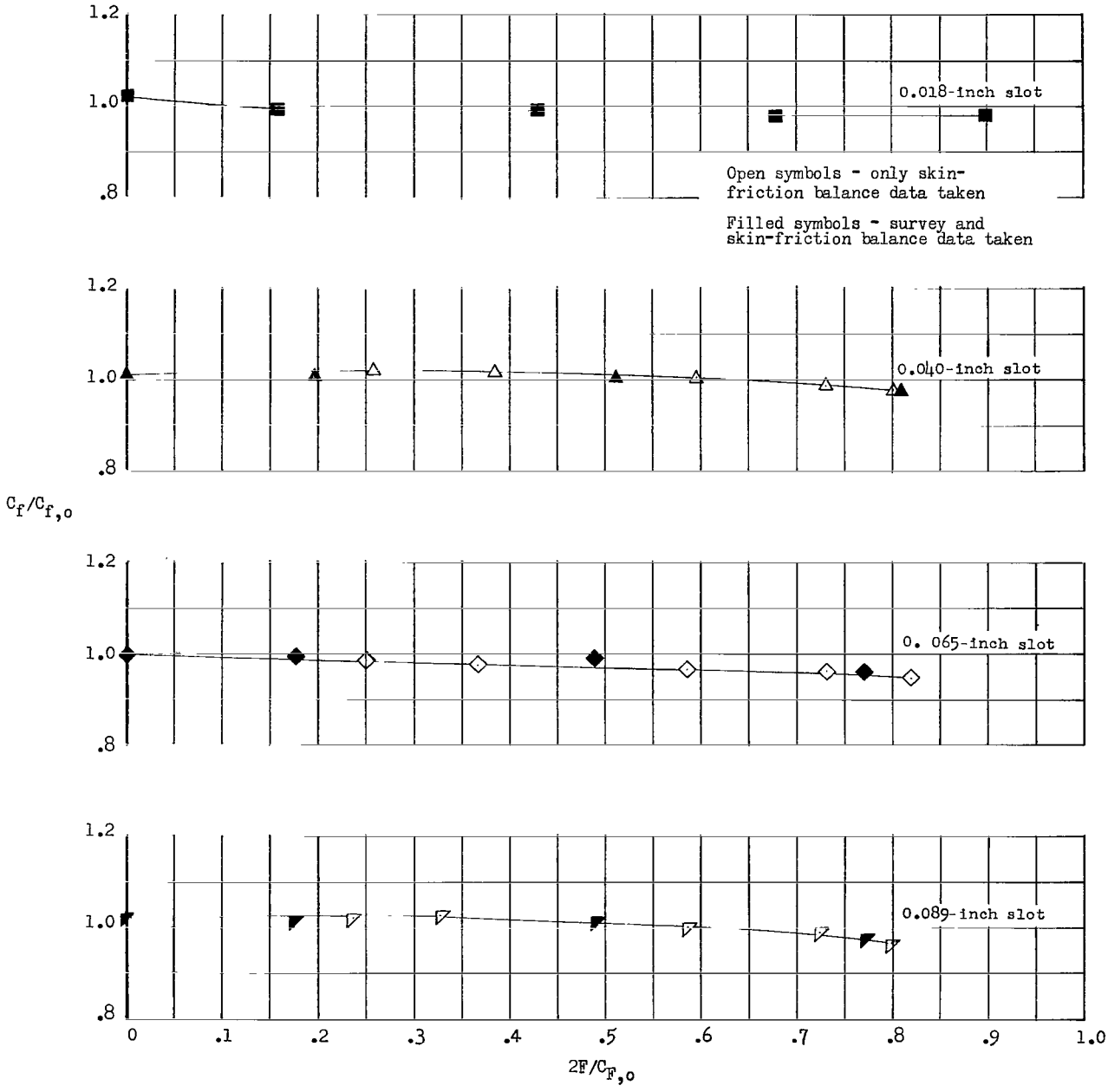

Figure 14.- Local skin-friction-coefficient ratio for different mass-flow rates for the flush-slot configuration. x = 20 inches.

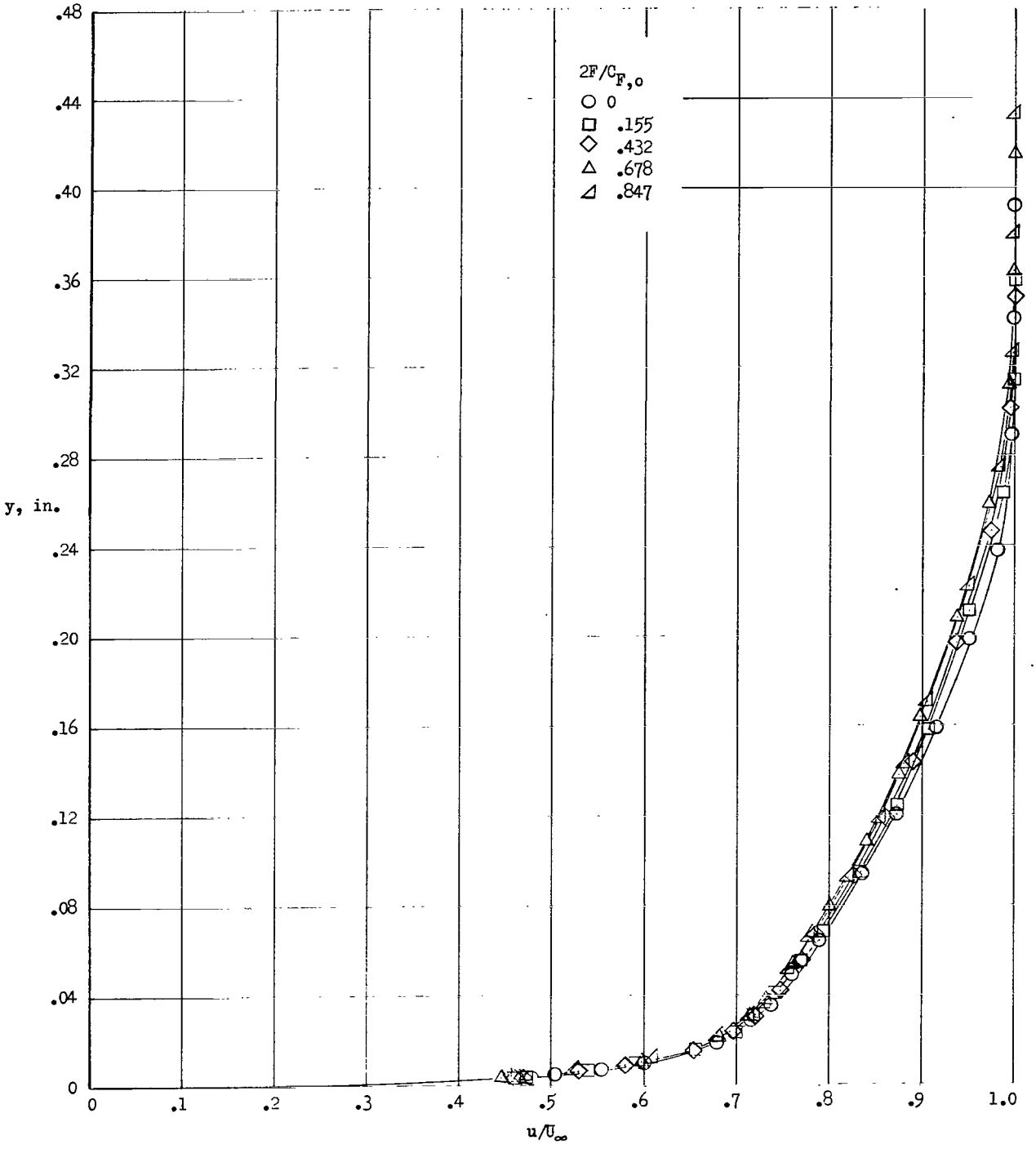

(a) 0.018-inch flush slot.

Figure 15.- Velocity profiles with injection. x = 19.325 inches.

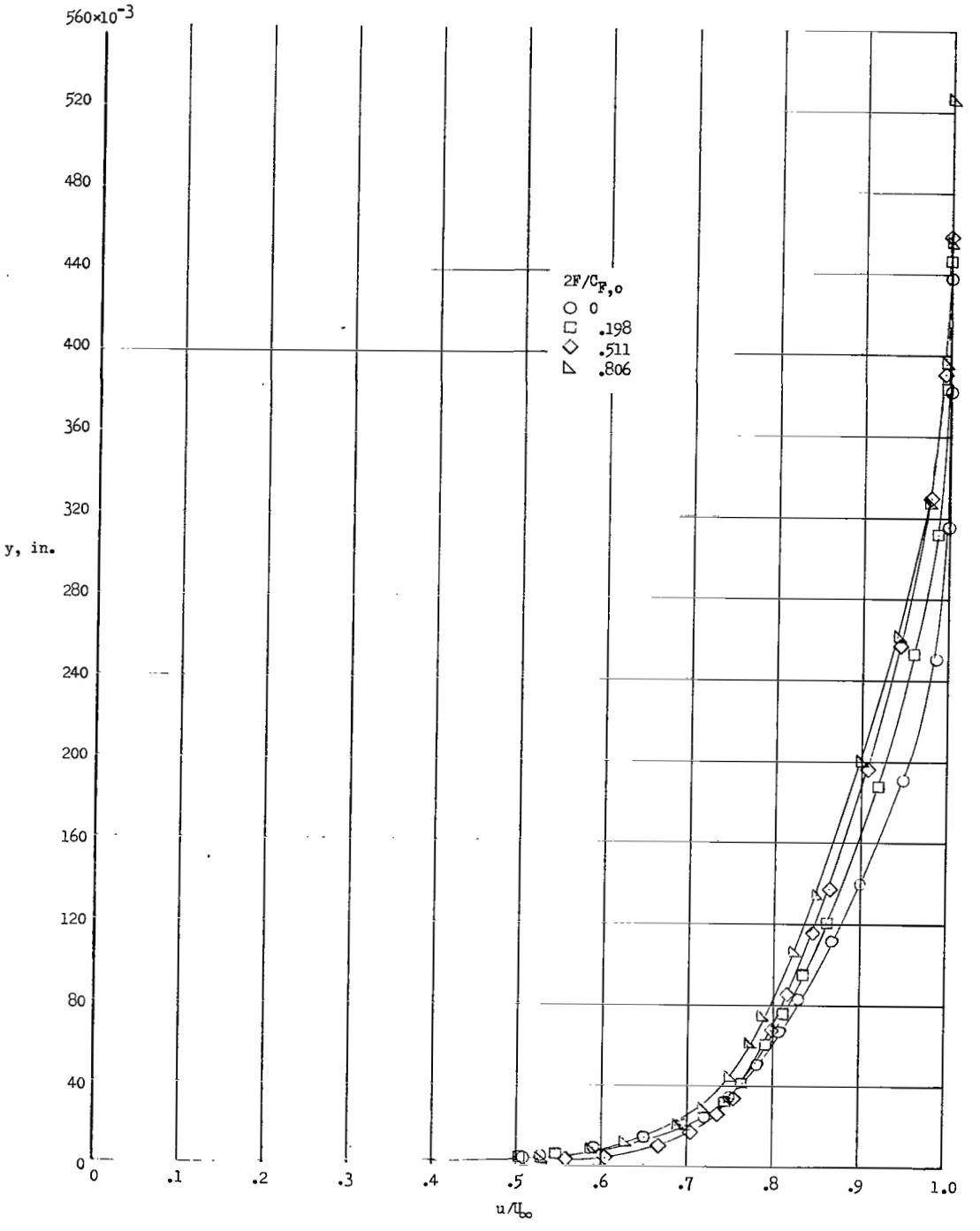

(b) 0.040-inch flush slot.

Figure 15.- Continued.

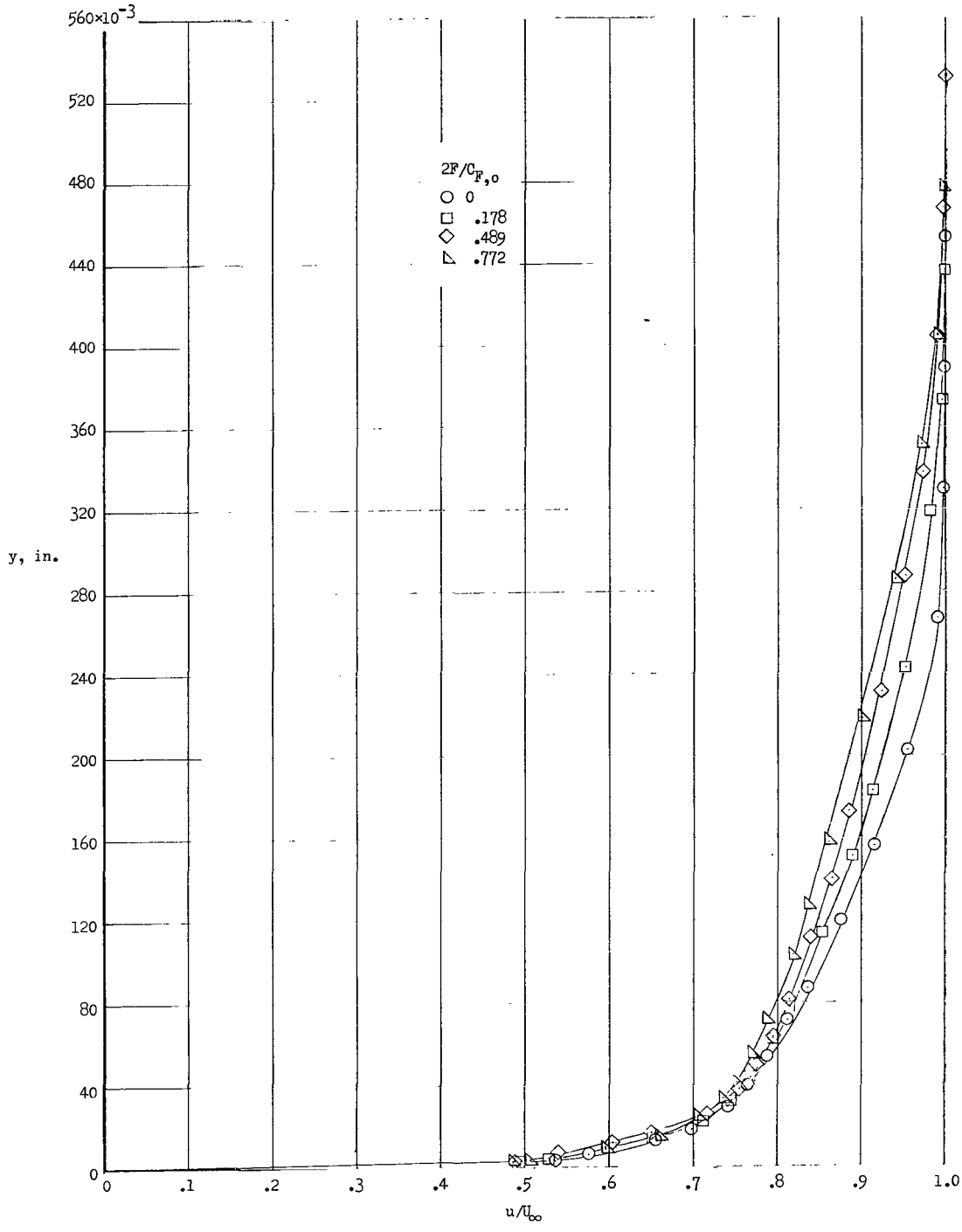

(c) 0.065-inch flush slot.

Figure 15.- Continued.

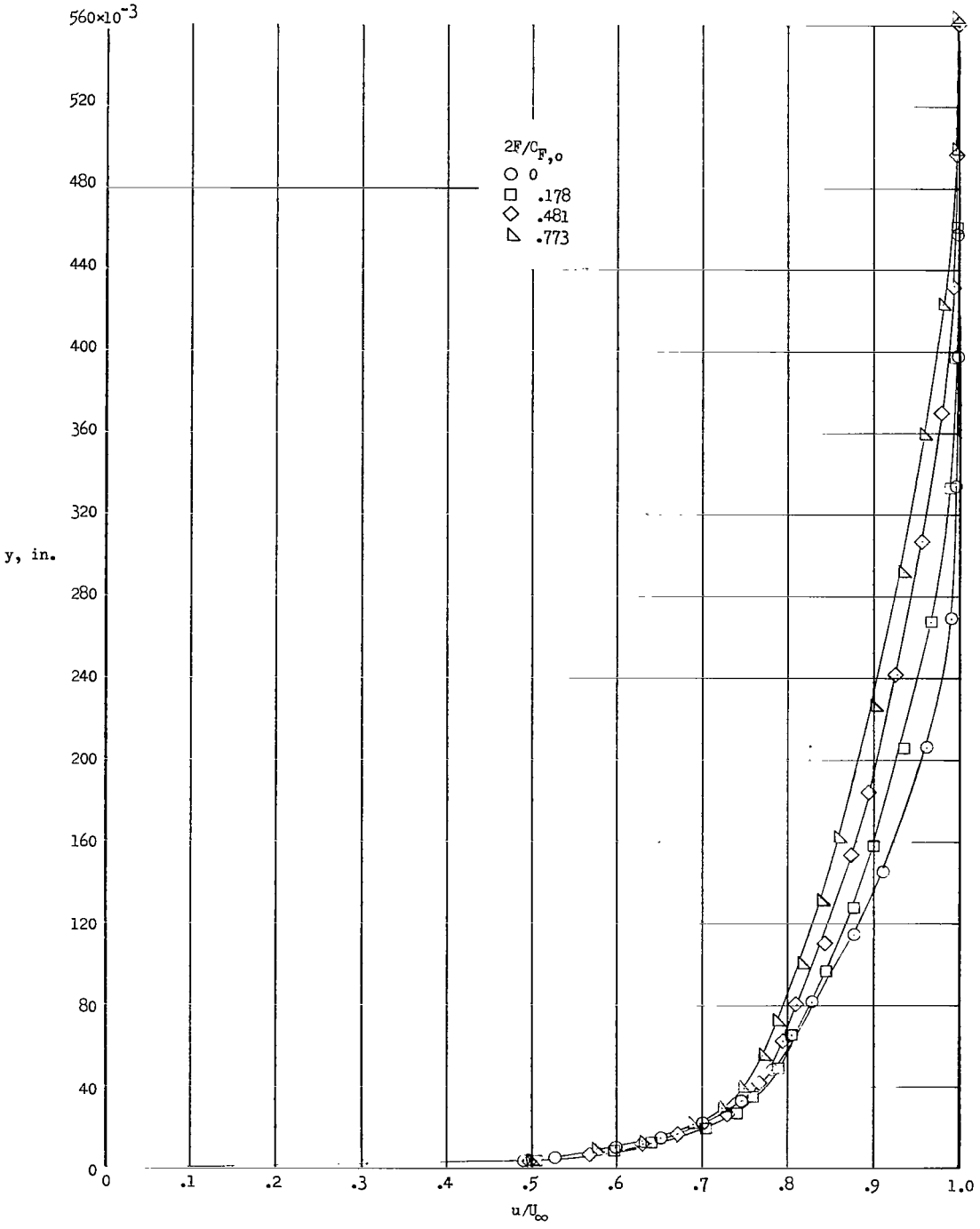

(d) 0.089-inch flush slot.

Figure 15.- Concluded.

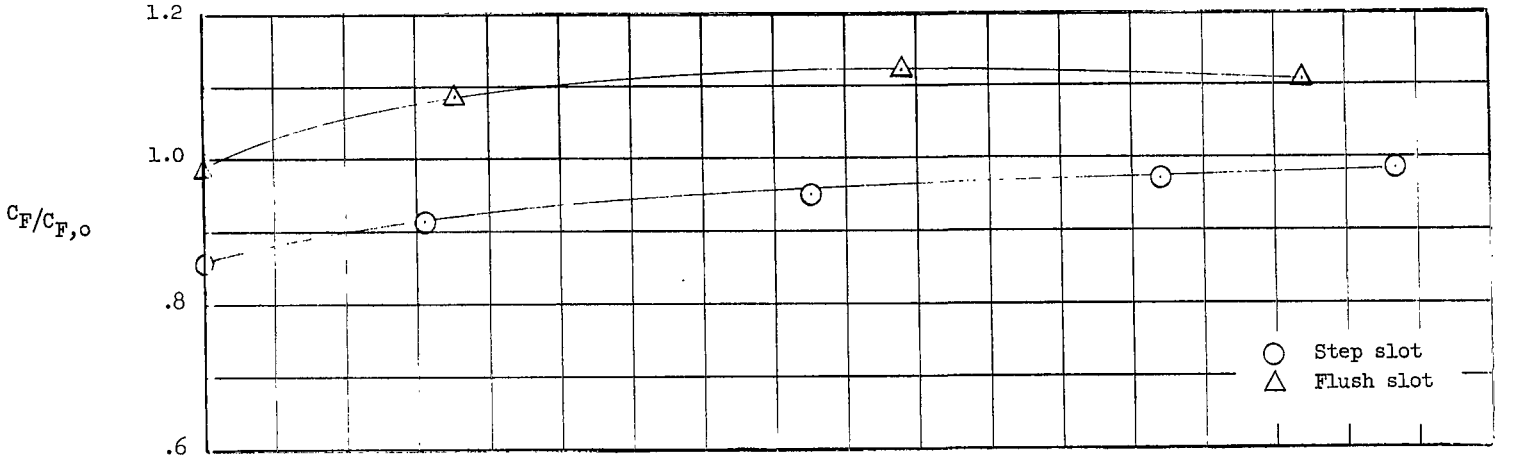

(a) Average skin-friction-coefficient ratio. x = 19.325 inches.

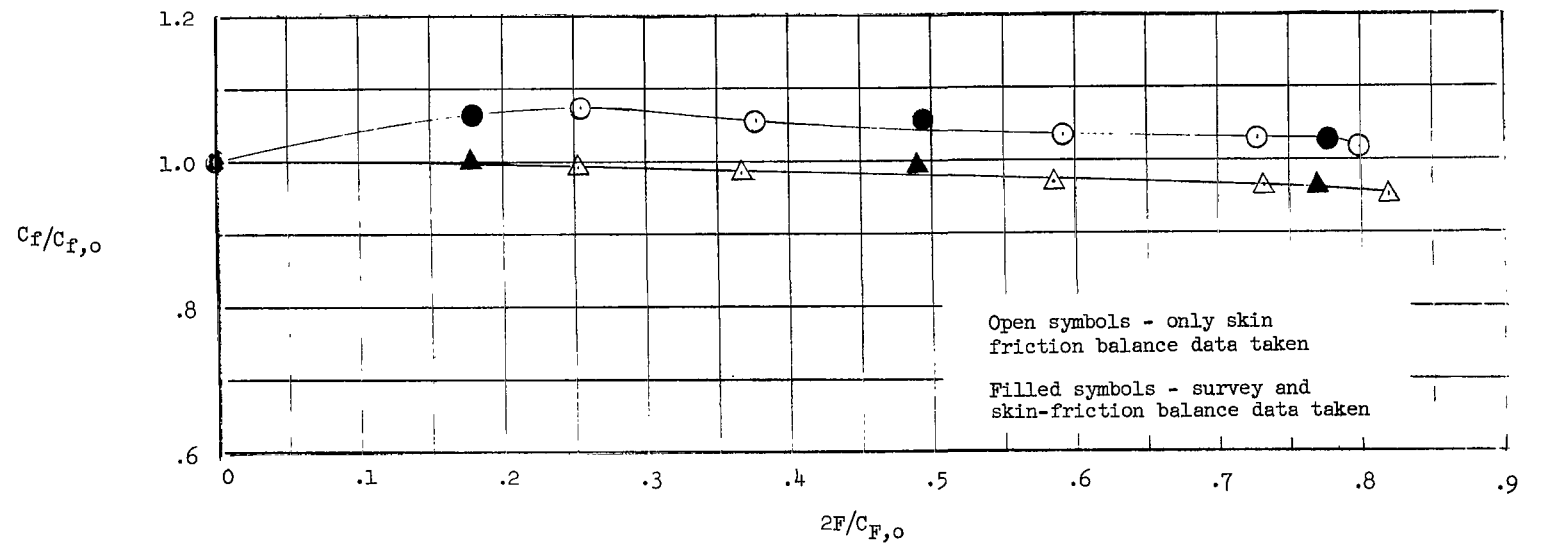

(b) Local skin-friction-coefficient ratio. x = 20 inches.

Figure 16.- Average and local skin-friction-coefficient ratios for 0.068-inch step slot and 0.065-inch flush slot.

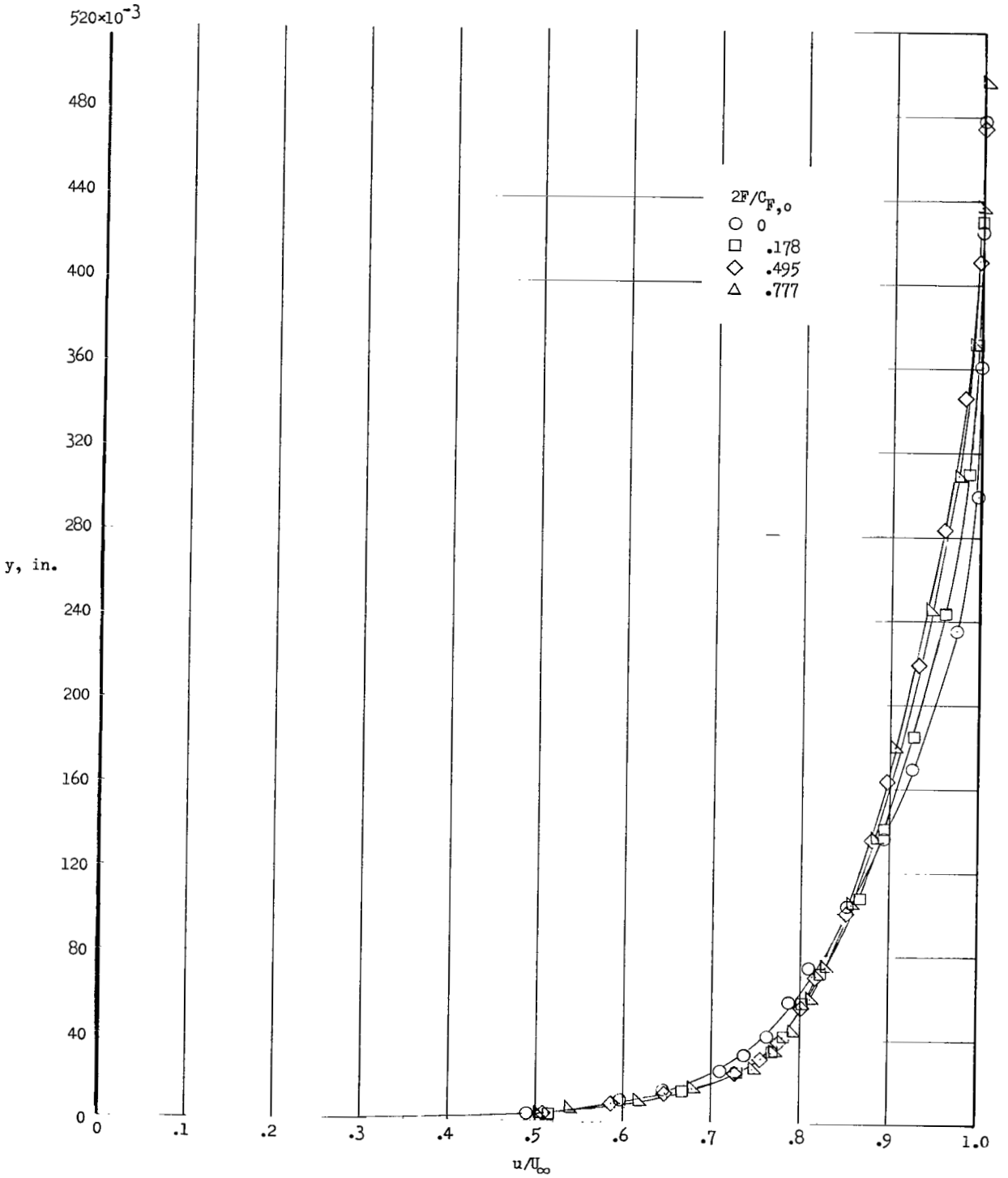

Figure 17.- Velocity profiles with injection for the 0.068-inch step slot. x = 19.325 inches.

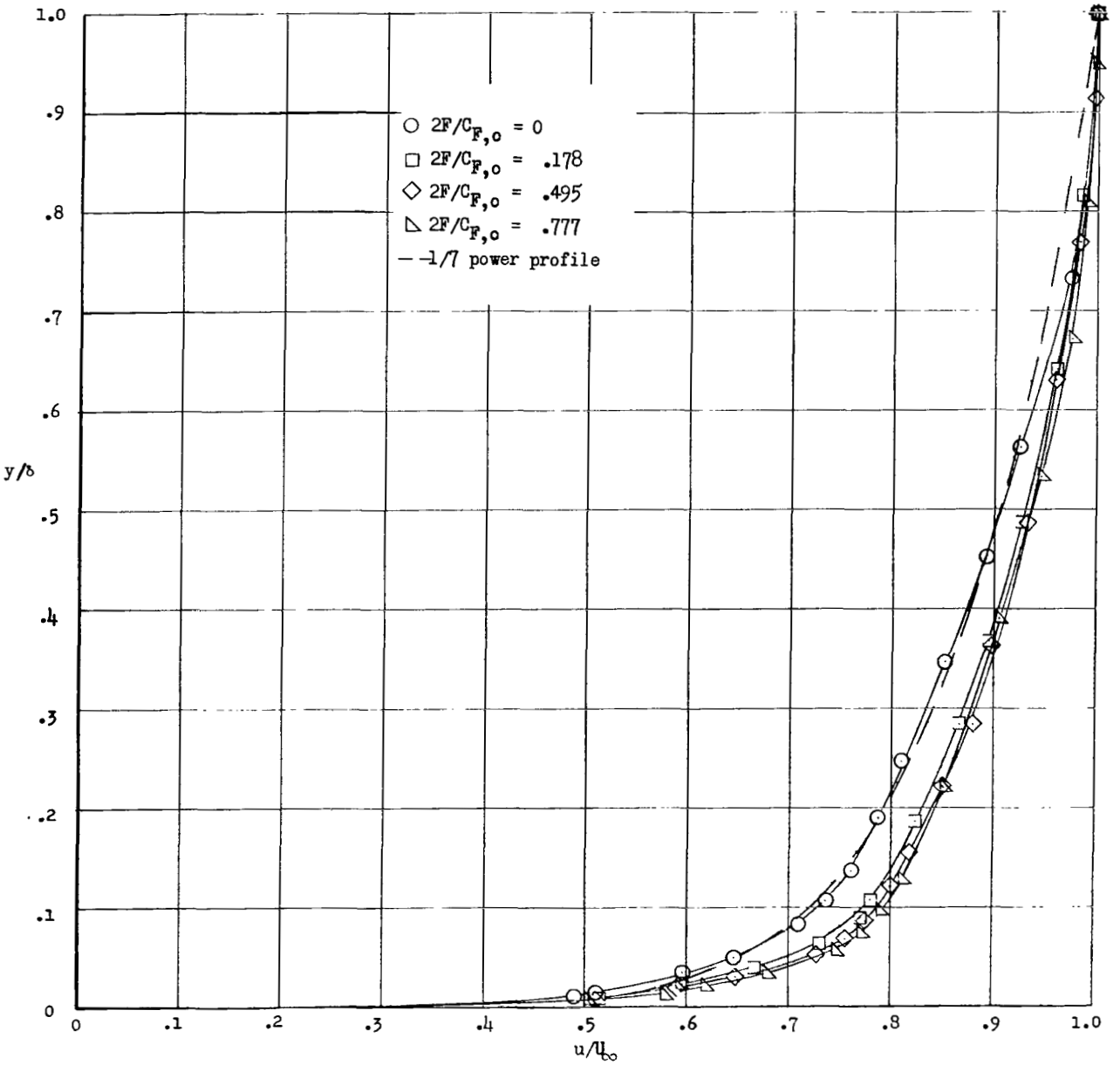

Figure 18.- Comparison between the 1/7-power profile and the velocity profiles for the 0.068-inch step slot. x = 19.325 inches.

2/7/85
96

"The aeronautical and space activities of the United States shall be conducted so as to contribute . . . to the expansion of human knowledge of phenomena in the atmosphere and space. The Administration shall provide for the widest practicable and appropriate dissemination of information concerning its activities and the results thereof."

—NATIONAL AERONAUTICS AND SPACE ACT OF 1958

NASA SCIENTIFIC AND TECHNICAL PUBLICATIONS

TECHNICAL REPORTS: Scientific and technical information considered important, complete, and a lasting contribution to existing knowledge.

TECHNICAL NOTES: Information less broad in scope but nevertheless of importance as a contribution to existing knowledge.

TECHNICAL MEMORANDUMS: Information receiving limited distribution because of preliminary data, security classification, or other reasons.

CONTRACTOR REPORTS: Technical information generated in connection with a NASA contract or grant and released under NASA auspices.

TECHNICAL TRANSLATIONS: Information published in a foreign language considered to merit NASA distribution in English.

TECHNICAL REPRINTS: Information derived from NASA activities and initially published in the form of journal articles.

SPECIAL PUBLICATIONS: Information derived from or of value to NASA activities but not necessarily reporting the results of individual NASA-programmed scientific efforts. Publications include conference proceedings, monographs, data compilations, handbooks, sourcebooks, and special bibliographies.

Details on the availability of these publications may be obtained from:

SCIENTIFIC AND TECHNICAL INFORMATION DIVISION

NATIONAL AERONAUTICS AND SPACE ADMINISTRATION

Washington, D.C. 20546